UNIVERSIDADE DE LISBOA
FACULDADE DE CIÊNCIAS

DEPARTAMENTO DE BIOLOGIA VEGETAL

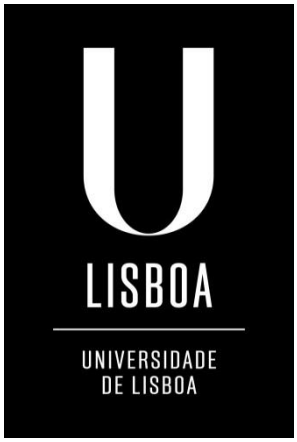

Testing the Mechanosensory versus Chemosensory hypotheses in left-right early development

Catarina Gonçalves Fonseca

Dissertação
Mestrado em Biologia Molecular e Genética

2013

UNIVERSIDADE DE LISBOA
FACULDADE DE CIÊNCIAS

DEPARTAMENTO DE BIOLOGIA VEGETAL

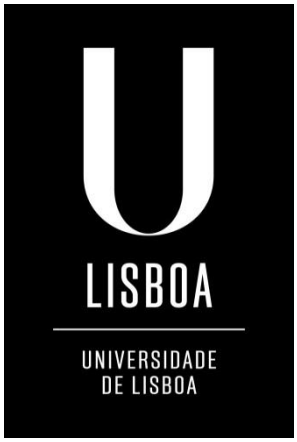

Testing the Mechanosensory versus Chemosensory hypotheses in left-right early development

Catarina Gonçalves Fonseca

Dissertação
Mestrado em Biologia Molecular e Genética

Dissertação orientada por:

Doutora Susana Santos Lopes (orientação externa)
CEDOC – Faculdade de Ciências Médicas da Universidade Nova de Lisboa

Professor Doutor José Feijó (orientação interna)
Faculdade de Ciências da Universidade de Lisboa

2013

ACKNOWLEDGMENTS

I want to start by thanking to Susana Lopes for the opportunity she gave me by accepting me in *Cilia Regulation and Disease* Lab, giving me the chance to work in a very interesting research area, new for me, and for her help when I needed

I also want to thank to Petra and Bárbara for all the things they taught me and their patience to teach me. Thank you for support and help during this year. I also want to thank to Monica, Pedro and Joana for help me in these lasts weeks, and by their availability ever. This thesis was only possible due to your help and support. It was a pleasure to work with you all.

I also want to thank to Professor Dr. José Feijó to accept my co-supervising.

I also want to thank to ‘’Grupo do Canto’’ (Petra, Claudia Q., Claudia P., Sofia, João, Pedro, Telmo, Neuza, André, Maria and Ângela) for all the moments spent in and outsider the lab. I also want to thank for all the given suport and advises given throughout this year, mainly in this last days. I will not Forget you.

A special thanks to Filipa, Susana Jéssica and Melanie for all the friendship throughout these years and for the good moments at coffees in the weekends.

I also want to thanks to João, Marília and Filipa for their friendship throughout this last three years and for all the support given and, principally to João for his motivating sayings.

A special thanks to João Donato that has always given me support and has been on my side when I needed the most, without never let me lower my arms and make me believe in myself.

For last, but the most important people, I want to thank to my parents, Otília and José for all the support and trusting that they deposited in me throughout my academic route. Without them nothing of this would be possible. I also want to thank to my sister Joana for the good sister she is and for believing in me, supporting me and because of our interesting conversations at the weekends.

ABSTRACT

Cilia are antenna-like organelles that protrude out of nearly all vertebrate cells. Two types of cilia can be defined: motile cilia, involved in moving fluids and primary cilia (shorter and immotile) that have sensory and signalling functions. Motile ciliary dysfunctions cause specific ciliopathies that affect mainly the respiratory tract, fertilization and left-right (LR) body establishment. The embryonic node is a ciliated structure where motile cilia generate an important fluid-flow named Nodal Flow (necessary for LR axis formation). Correct left-right patterning sometimes fails during development and defects, such as *situs inversus* occur. The correct left-right axis formation is highly dependent on signalling pathways downstream of such directional fluid-flow. The mechanism by which this process occurs is still unknown but there are supporting data in the field both for mechano and chemosensory pathways. There are two models that try to explain the mechanism by which LR is transferred to the Lateral Plate mesoderm. The “Morphogen model” – defends that morphogens become concentrated in left side of the node in response to flow. The other model, known as the “Two-cilia model” suggests that two different cilia types in the node perform different functions. From an unpublished microarray data we chose two genes in order to study these two models in zebrafish. “Morphogen Model” was studied with *Tas1r1*, because it has been recently reported that Tas1R receptors are expressed in ciliated epithelia acting as chemosensors. The “Two-cilia model” was studied with the *pkd1* gene, because in kidney ciliated cells was described that Pkd1 interacts with Pkd2 originating a mechanosensor complex important for kidney homeostasis. Knockdown of both genes with morpholino technology was used (independently) in order to observe if the lack of these genes caused left-right defects. Results showed that *tas1r1* knockdown does not seem to generate any LR defects. Regarding *Pkd1* we could not make definitive conclusions because the morpholino we designed was in a projected sequence.

RESUMO

Os cílios são organelos semelhantes a antenas que se projetam para fora da célula em todas as células de vertebrados. Existem dois tipos de cílios que são classificados de acordo com a sua função: cílios móveis, que estão envolvidos no movimento de fluidos e cílios primários (mais pequenos e imóveis) que têm funções sensoriais e sinalizadoras. Dependendo da sua função e localização nos epitélios ou órgãos a estrutura ciliar é também diferente. Alterações ao nível da motilidade ciliar causam doenças específicas do cílio que afetam principalmente o aparelho respiratório, a fertilização e o estabelecimento da assimetria esquerda-direita do corpo. O nó embrionário, também conhecido como organizador da esquerda-direita do embrião vertebrado, é uma estrutura ciliada onde os cílios móveis originam um importante fluxo de fluido, chamado de Fluxo Nodal (necessário para a formação do eixo esquerdo-direito). Por vezes há falhas na correta formação do padrão esquerdo-direito durante o desenvolvimento que levam ao aparecimento de defeitos como situs inversus. O mecanismo pelo qual este processo ocorre é ainda desconhecido mas existe informação na área que suporta duas vias: mecano-senora e quimio-sensora. Assim, existem dois modelos que tentam explicar como é que ocorre a ativação da expressão de genes assimétrica e como é que esta informação é transferida para a placa lateral da mesoderme. O “Modelo dos Morfogénios” defende que determinados morfogénios são transportados do lado direito para o lado esquerdo do nó, em resposta ao fluxo nodal e ficam concentrados do lado esquerdo onde iniciam uma sinalização intracelular. O outro modelo, conhecido como “Modelo dos Dois tipos de Cílios”, sugere que existem dois tipos de cílios diferentes a desempenharem funções distintas no nó. Este modelo foi baseado na descoberta de que no nó embrionário do rato existem cílios móveis, na zona central, identificados pela presença de dineínas (proteínas motoras que conferem o movimento ciliar), mas também existem cílios imóveis a cercar os cílios móveis. Estes cílios imóveis foram localizados por imunofluorescência na zona mais periférica do nó, também conhecida por região perinodal. Ambos os modelos descrevem que a libertação de Ca^{2+} intracelular do lado esquerdo do nó é um fator essencial para a ativação da expressão assimétrica de genes envolvidos no estabelecimento do padrão esquerdo-direito.

A partir de dados novos, ainda não publicados, obtidos após a análise de resultados de uma experiencia de expressão genética usando microarrays, feita no nosso laboratório, foram escolhidos dois genes de acordo com a sua expressão na vesicula de Kupffer (orgão análogo ao nó do rato, importante também no estabelecimento da assimetria esquerda direita no peixe zebra e medaka). Usaram-se embriões selvagens (wt) e mutantes *deltaD*$^{-/-}$ para podermos comparar as diferenças de expressão nestas duas condições em embriões

de peixe zebra. Um dos genes escolhidos foi o *tas1r1* (pertencente à família de recetores de sabor Tas1R normalmente expressos no bolbos gustativos da boca). Uma vez que, tinha sido descrita a sua expressão em epitélios ciliados e espermatozoides, atuando como sensores químicos. O outro gene escolhido para o estudo foi o *pkd1* porque tinha sido descrito que nas células ciliadas do rim o Pkd1 interage com o Pkd2 de modo a formarem um complexo importante para a homeostase deste órgão. Deste modo, com o *tas1r1* fomos estudar o modelo dos Morphogenios e se este gene tem algum papel relevante como sensor-químico no cílio da vesicula de Kupffer. Por outro lado, com o *pkd1* fomos testar o modelo dos Dois Tipos de Cílios, de modo a tentar perceber se este também tinha um papel importante como sensor mecânico para o estabelecimento do padrão esquerdo-direito. Para tal utilizamos a tecnologia de injeção de morpholino de modo a eliminar a tradução destes dois genes (independentemente) para avaliarmos se a sua ausência leva ou não a defeitos de lateralidade no desenvolvimento embrionário.

Antes de iniciar esta experiência procedemos à confirmação da *microaray* através da técnica de qPCR em embriões wt e mutantes para o pkd1 e para embriões wt a diferentes estadios (10 hpf, 13 hpf e 4 dpf) de modo a validar a expressão do tas1r1.

Para confirmar se ambos os genes têm um papel importante para o estabelecimento do eixo direito-esquerdo do corpo, procedeu-se à avaliação da posição dos órgãos internos, nomeadamente o coração (às 30 horas) e o fígado e pâncreas (às 50 horas). Para o coração os embriões, vivos, foram vistos à lupa, a qual permitiu que se observasse o bater do coração por baixo do olho esquerdo (para embriões normais), do olho direito ou entre os dois olhos para embriões com defeitos de lateralidade. O fígado e pâncreas foram observados de duas formas distintas, umas delas foi usando uma linha transgénica de peixe zebra foxj1a:GFP que marca estes dois órgãos a verde e por isso estes embriões foram visualizados vivos à lupa de fluorescência. A outra forma de avaliação foi pelo uso de sonda de hibridação *in situ* especifica para marcar estes dois órgãos.

Após a análise da posição destes três órgãos concluímos que os embriões não possuíam defeitos de lateralidade. Assim, seguimos o nosso estudo com a hipótese do modelo dos Dois Tipos de Cílios mas com outro gene, o *pkd2*, uma vez que já está descrita a sua importância a nível do estabelecimento do padrão esquerdo-direito no corpo. Além de analisar e confirmar o fenótipo já descrito ao nível dos defeitos de lateralidade observados pela posição do coração e do fígado e pâncreas, usando a tecnologia de injeção de morpholino, concluímos o nosso estudo com a avaliação da expressão de *pkd2* nos cílios da vesicula de Kupffer. Nestes estudos percebemos que a expressão de Pkd2 não é igual em

todos os cílios e que pode estar não só nos cílios imoveis, como descrito pela sua função mecano-sensora no nó do rato e na vesicula de kupffer do peixe medaka. Isto deixa em aberto a hipótese de que os cílios moveis poderão desempenhar funções sensoras além de funções de movimento e formação de fluxo na vesicula.

Como estudos futuros será importante obter um construto para expressar Pkd2 em embriões de peixe zebra vivos, através da injeção deste no embrião. Desta forma será possível fazer estudos de co-localização com arl13b-GFP que permitirão observar os cílios que estão em movimento e os cílios que não têm movimento, ao longo de toda a vesicula de Kupffer. Isto é possível devido ao facto da proteína Arl13b ser uma proteína de membrana e como tal está presente quer em cílios móveis quer em cílios imóveis. Deste modo ao fazermos esta experiência podemos perceber em que tipo de cílios se encontra o Pkd2 e a sua distribuição pela vesicula de Kupffer. Mais ainda, podemos tentar fazer estudos funcionais dos cílios móveis, de modo a perceber se realmente há ou não um papel deste tipo de cílios a nível mecano-sensor e qual a sua contribuição a nível sensorial no estabelecimento do correto padrão esquerdo-direito do corpo. Esta abordagem poderia ser feita pela supressão genética dos cílios imóveis de modo a perceber se os cílios móveis são suficientes para desempenhar a sua função de gerar o fluxo e ainda ter a capacidade de sentir os estímulos mecânicos gerados sem comprometer o estabelecimento do correto padrão esquerdo-direito do corpo.

Concluindo, o estudo feito nesta dissertação foi relevante na medida em que proporcionou novos dados relativamente à localização do Pkd2 no cílio e na vesicula de Kupffer, levando assim ao aparecimento de novas hipóteses que devem e têm de ser testadas no futuro.

INDEX

LIST OF FIGURES

Annex:

LIST OF TABLES

Annex:

1. INTRODUCTION

1.1. Cilia re-discovered

Cilia, also known as flagella, are microtubule-based organelles[1] found on almost all vertebrate cells[2]. Cilia are highly conserved organelles and the oldest known cellular organelle described for the first time in 1675 by Anthony van Leeuwenhoek on ciliated protozoa[3]. These organelles project from the surface of almost all cell types in vertebrates[4], both as embryos and adult bodies[5]. For many decades the investigators gave no importance to these organelles until they understood its importance, function and contribution of ciliary dysfunction to human genetic diseases[6]. They play an essential role in signal transduction, physiological roles during development, cellular homeostasis, regulating also intracellular calcium levels and Wnt and Hedgehog signaling pathways[5]. Cilia also carry out diverse sensory functions including the detection of light, odor and fluid flow, or are motile and are responsible for moving cells over substrates or moving fluids over epithelial surfaces[4].

1.2. Cilia

Cilia are generated during interphase, when cells exit the cell cycle from mitosis into a stationary or differentiated state and are reabsorbed when cells entry again into the cell cycle[7,8]. In this process, called ciliogenesis, cilia emerge from a plasma membrane-associated foundation called basal body that templates the nucleation of the axoneme, the structural core of cilia that consist of nine doublets of microtubules[8]. The basal body is also made by microtubules, nine triplets of microtubules (Figure 1.1). Between the basal body and ciliary body exists a transition zone, which starts where the triplet microtubules end and where the axoneme of cilia begins (Figure1.1). In combination with the internal structure of basal body, it is thought that the transition zone acts as filter for the cilium, regulating the molecules that can pass into or out of the cilium[9]. The ciliary tip is another part of the cilium that contains a specialized protein complex[1]. This structure is an important region to axonemal growth and reabsorption, and is thought to be a main point of regulation and remodeling of intraflagellar transport (IFT)[7]. This transport is needed to move the organelle´s structure components from cell body to ciliary tip and then to return proteins from the cilium to the cell body (anterograde transport is done by the motor subunit kif3 and retrograde transport by dynein motors) (Cole 1993), once the proteins for cilia assembly and function are synthetized in cell body and not in cilia[11].

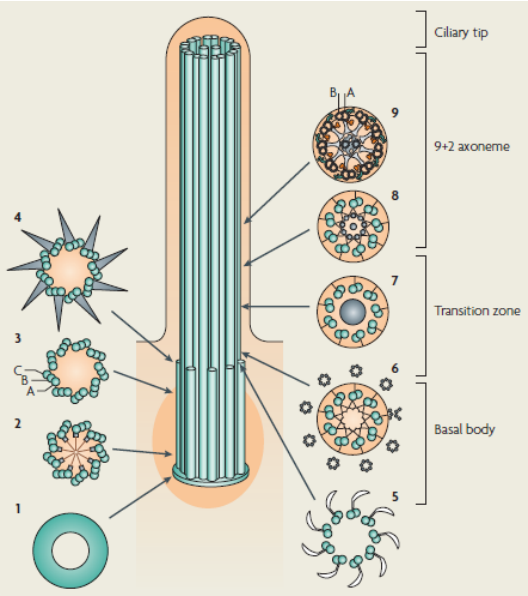

Figure 1.1 Cilia subcompartments
Scheme of a cross section of the microtubular structure in each subcompartment of cilia: Basal body (1-4) – 9 x 3 microtubular structure; Transition zone (5-8) – converts the triplet microtubular structure of the basal body into the axonemal doublet structure; Axoneme (9) – 9+2 doublet microtubular structure; and Ciliary tip and (Fliegauf *et al* 2007)

1.2.1. Types of cilia

According to the axonemal structure of cilia, its function and its ability to move, they can be classified into two groups: Primary and Motile cilia.

Primary cilia are typically short and immotile and are present on almost vertebrate cell types[8] as a single copy per cell[12]. These types of cilia have a 9+0 axoneme, so they do not have a central pair of microtubules and lack inner (IDAs) and outer (ODAs) dynein arms. The absence of dynein arms and radial spokes makes them immotile.

Primary cilia were long thought to be vestigial, but were recently found to act as a complex signaling center, because a high concentration of signaling molecules were found near this type of cilium. Many of cilia are highly adapted to serve specialized sensory functions[13]. They participate in numerous biological process ranging from chemo and mechanosensation to the transduction of an expanding list of signaling cascades, that are essential to regulate cellular and tissue homeostasis[8]. Moreover, cilia are organelles functionally very important, involved in a growing list of diseases caused by defects at its level, such as, PKD (polycystic kidney disease) BBS (Bardet-Biedl syndrome), Joubert Syndrome and others (Goetz & Anderson 2010).

Motile cilia are usually longer and the presence of dynein arms confers them the possibility to beat [14]. The axoneme of motile cilia is composed of nine peripheral microtubule doublet and two central microtubules (the central pair),[15] so they have a 9+2 axoneme[12,16].

The motility of these cilia depends on the presence of IDAS and ODAs, that are attached to the microtubules, the dynein regulator complex (DRC), radial spokes[15] and central pair

projections[12]. Motile cilia have also nexin links that are responsible for the connection of microtubules doublets[7] and the constraints caused by inter-doublet sliding translate into ciliary bending [6].

In mammalians, motile 9+2 cilia normally concentrate in large numbers on the cell surface and beat in an orchestrated wave like fashion being involved in fluid and cell movement[13]. Motile cilia are responsible for the generation of fluid-flow over epithelia such as mucus clearance in the respiratory tract and circulation of cerebrospinal fluid within the brain and spinal cord[14]. Thus, traditionally, motile cilia were thought not to be involved in sensory mechanisms.

However, recently, some studies have described the possibility that motile cilia also possess sensory skills, which means that functional differences between these two types of cilia are not as strictly demarcated[17]. Moreover, it has been described that there are many exceptions on this definition that favor the distinction into four subtypes: motile 9+2 cilia (respiratory and ependymal cilia), motile 9+0 (nodal cilia in node mouse that create a leftward flow of the surrounding fluid and this flow is essential for left-right development[18], immotile 9+2 (kinocilium of hair cells) and non-motile 9+0 (renal monocilia and photoreceptor-connecting cilia)[7].

1.3. Ciliopathies

As already mentioned, cilia are present in almost all organs of the human body, and there is increasing evidence that dysfunction of cilia are involved in many different human disorders[16], called ciliopathies, like polycystic kidney disease (PKD) and primary cilia dyskinesia (PCD)[7,19]. The ciliary defects can occur at structural level or in protein localization [19] and in motile or immotile cilia. A ciliopathy that affects immotile cilia is PKD or Autosomal dominant PKD (ADPKD) by mutations in two genes: *pkd1* and *pkd2*, and is related with defects is $Ca2^{+}$ signaling[20]. This disease is a devastating common genetic disorder, with an estimated prevalence of between 1:400 and 1:1000 individuals[21]. PKD is characterized by defects in renal epithelial cells, leading to an increase of cell proliferation and cyst formation in kidney, liver and pancreas[22,23].

Besides causing cysts formation, PKD is related with ciliary defects and in this disease, many ciliary proteins, localized to the ciliary membrane or basal body, are disrupted [24]. The disruption of ciliary proteins influence the Ca^{2+} signaling mediated by Pkd2, leading to a relation between ciliary signaling and cyst formation [25]. This topic will be discussed further ahead.

Dysfunctions in motile cilia are more specific, with major manifestations in mammalians as early embryonic death due to failure of embryonic turning, respiratory dysfunction, reproductive sterility and hydrocephalus [26]**.** An example of a disease that affects the motile cilia is the PCD, firstly identified by Afzelius in 1976 [27]. This disease is characterized by bronchiectasis, infertility and defects in body situs, as *situs inversus*. This triade of symptoms is called the Kartagener syndrome. Patients with PCD have mutations in dynein arms as DNAH1 and DNAH5, that are necessary for ciliary motility in order to generate nodal flow and to allow normal mucociliary clearance (absent in PCD patients) [16]. Moreover, half of individuals with PCD exhibit *situs inversus totalis* (which is consistent with randomization of left-right (LR) asymmetry). This observation primed Afzelius (1976) to first hypothesize that cilia motility was important in the establishment of LR body asymmetry. But how this regulation is made, will be discussed below [28] .

1.4. Cilia in left-right establishment

The generation of LR asymmetry occurs in two key steps. The first step is characterized by symmetry-breaking in the node. Here, an asymmetric signal that is generated in the node is transferred to the left side of the lateral plate mesoderm (LMP). This transference leads to an asymmetric expression of the gene *nodal* in the left LPM, which correspond to the second step [29].

In normal mouse embryos, nodal cilia rotate in a clockwise direction and create a leftward fluid flow (nodal flow) which influences the asymmetric cascade of gene expression, that moves across the node (Okada 2005). The mouse node or the homologue Kupffer's vesicle (KV) in zebrafish are transient organs present only in the first stages of embryonic development [31] and they are common among vertebrates (Lourenço and Saúde, 2010). The mouse node is a cavity filled with extra embryonic fluid and the zebrafish Kupffer´s vesicle is a elipsoid vesicle also full with fluid at the tailbud region (Figure 1.2)[31]. These organs are constituted by monociliated cells, and whereas in mouse cilia protrude from cells located on the ventral side of the node into the node cavity [33], in zebrafish cilia are all around the cavity[34].

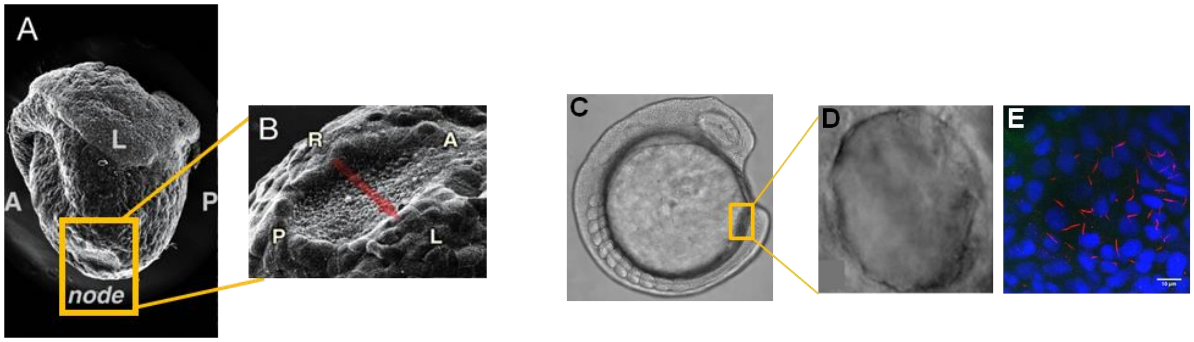

Figure 1.2 Vertebrates left-right organizer
Scanning electron micrographs of the mouse node at 8.0 days post coitum **(A)**. In higher magnification view are the ventral node cells (B). The anteroposterior and left-right axes are indicated by A/P and L/R, respectively (Adapted by Hamada 2008). Light microscopy image of a live zebrafish embryo at 13.5 hpf (9 somites stage) **(C)**. Kupffer´s Vesicle is shown in higher magnification by: high resolution DIC microscopy **(D)** and confocal microscopy of all z-sections spaced 0.5 µm apart (in red *alexa*546), cilia labeled with anti-acetylated α-tubulin; and in blue (DAPI) the monociliated cells´ nuclei **(E)**; white bar – 10 µm (Adapted from Lopes 2010)

The nodal flow generated by nodal cilia leads to a transference of information to the left side of the node and subsequently to the asymmetric expression of *nodal* on the left side of LPM[29,35]. In LPM, *nodal*, exerts a positive feedback on itself and will activate its own negative regulators, the *lefty* genes[32]. *lefty1* is expressed in the midline and prevents the nodal activation on the right LPM and *lefty2* is expressed on the left LPM and restricts the domain of *nodal* expression into the prospective heart region [29,32]. Absence of *lefty* genes leads to a symmetric *nodal* expression in LPM, which influences normal internal organ positioning. *Nodal* expression in LPM also activates the transcription factor Pitx2, which is expressed on the left side of LPM. This transcription factor persists until later stages, maintained by Nkx2, and is responsible for the regulation of asymmetric organogenesis[29]. Mice that lack Pitx2 exhibit laterally defects in most visceral organs[29]. Likewise, other mutants have been crucial to the interpretation of the left-right cascade of events.

The *iv* (*Inversus viscerum*) mouse embryos have a mutation in motor protein left-right dynein (lrd), only present in nodal cells that leads a loss of motility of motile nodal cilia. The absence of motility results in the absence of nodal flow and consequently leads a randomization in LR asymmetry. This finding indicates that nodal flow is necessary for the establishment of the LR body axis[36–38], Furthermore, Nonaka *et al* (2002) showed that an artificial generated nodal flow to the right side of the node, independent from ciliary motility, is sufficient to reverse the laterality markers on the LPM[39].

1.4.1. The two model to explain the LR establishment

In order to explain how LR establishment occurs, there are two theoretical models proposed, based on some experimental data. The “morphogen model” proposes that morphogens become concentrated on the left side of the node in response to flow[18,40], while the other

model, the so called “two cilia model”, suggests that there are two types of cilia in the node that perform different functions [41,42]

The Morphogen model was proposed by Nonaka and co-workers,[18] who saw that in the mouse node there was a leftward fluid flow that they named as nodal flow (Figure1.3). From this observation they proposed that there was a putative secretory factor that was being concentrated on the left-side of the mouse node leading to activation of signaling pathways on this side of the node[18,36]. In 2005, Tanaka and co-workers identified membrane-sheathed objects, that they termed “nodal vesicular parcels” (NVPs), which carry Sonic Hedgehoc (SHH) and Retinoic acid (RA). They saw that when they abolished the fibroblast growth factor (FGF) pathway, they observed a reduction of Ca^{2+} signaling on left side of the node that was rescued when SHH and RA were added[40]. They also showed that FGF signaling triggered the secretion of these NVPs that are transported to the left side by nodal flow and are fragmented on the ciliated surface releasing their contents in proximity to the left wall[40]. This process was thought to lead to an activation of the downstream signaling pathways starting with an elevation of Ca^{2+} levels on the left side[40], thus starting symmetry breaking [7]. The symmetry breaking is declared based on asymmetric expression of mRNAs for signaling molecules in the LPM, such as Nodal, Lefty2 and transcription factor Pitx2[7]. The Physicists Cartwright and co-workers, based on Tanaka´s findings, modeled the movement of the NVPs across the node and demonstrated that the flow should indeed cause them to accumulate on the left side of the node, as necessary for symmetry breaking[43]. However, they studied also the rupture of NVPs and reported that the rupture cannot be triggered by flow forces and must be induced by an as yet undiscovered biochemical mechanism[43].

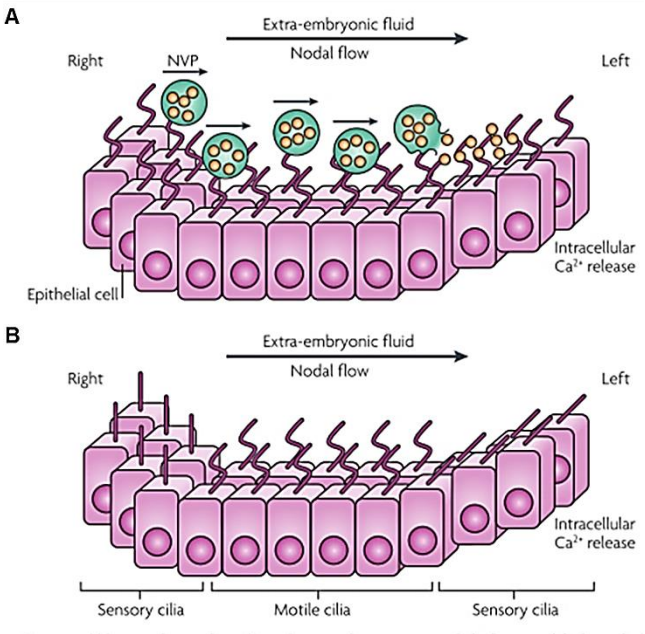

Figure 1.3 Current models of the LR establishment
The morphogen model **(A)** argues that nodal vesicular parcels (NVPs) full of retinoic acid and sonic hedgehog are secreted from the right side of the node and transported by nodal flow to the left side. Here NVPs are smashed, releasing their content. By enhancing intracellular Ca^{2+} levels in node left side cells, an asymmetric gene expression is induced. The Two cilia model **(B)** defend that there are two types of cilia (motile and immotile) in the node. Motile cilia, in the centre of node, generate a leftward nodal flow that is mechanically sensed by immotile cilia present in node periphery. Bending of immotile cilia leads to intracellular Ca^{2+} realize in left side of the node that activates an asymmetric gene expression (Fliegauf 2007).

The alternative model, the 'two cilia model' or mechanosensory model was proposed by McGrath and co-workers in 2003 when they observed two different populations of monocilia in the mouse node. They identified that cells located centrally in the node had motile monocilia that expressed both the motor protein: left-right dynein (Lrd) and the cation channel Pkd2, whereas those cells in periphery of the node had immotile monocilia that contained only Pkd2[41]. This model proposes that the motile cilia present at the center generate the leftward fluid flow, and the immotile cilia located at the periphery of the node might detect this flow by mechanosensory mechanisms and initiate downstream calcium mediated events[16,41,42,44] (Figure 1.3).

A stronger support for the mechanosensory model was the finding that LR signaling in humans was disrupted by mutations in human polycystic kidney disease gene *pkd2*[45,46] . Mutations in Pkd2 had already been linked to randomization of left-right body asymmetry in mice[47]. A very important evidence for involving Pkd2 in mechanosensation was given by Nauli *et al*[48] when they reported that the primary cilia of renal epithelia cells without Pkd1 or Pkd2 triggered the appearance of cystic kidneys[48] In zebrafish KV, Essner *et al* [31] observed that KV cells are monociliated and upon injection of fluorescent beads they saw that KV cilia are capable of generating a consistent directional counterclockwise flow inside KV[31]. Moreover, the knockdown of lrd1 in zebrafish disrupts the fluid flow in KV, resulting in a randomization of nodal-related gene, *spaw*, expression in LPM and cardiac laterality which means that fluid flow is also required for a correct LR patterning in zebrafish, as in the mouse[31,49]. However it is not completely understood how (in zebrafish) fluid flow inside a closed vesicle triggers an asymmetric gene expression important for LR determination. However, it is known that this process also results in asymmetric calcium elevation on the left side of the KV[44,50]. In summary, both models are plausible and still apply to mouse and zebrafish model systems[13]. However new hypothesis have appeared and claim that all cilia (motile and immotile) have sensory functions[51]. Bloodgood and co-workers reported that motile cilia of mammalian respiratory epithelium and oviductal epithelium exhibit chemosensory proprieties[17]. Further studies are necessary to clarify the mechanism that determinates how LR axis patterning information is conveyed by fluid flow and, maybe, sensed by specialized cilia[13].

1.5. Objectives

In my project we proposed to study these two models using the zebrafish embryo and studying the role of two different genes. To test the mechanosensation (two cilia model) we

studied the *pkd1* gene that codes for the potential mechanosensor partner of Pkd2. In order to test the chemosensation (morphogen model) we used *tas1r1* gene that codes for a G-protein-coupled receptor (GPCR), and is a taste receptor from the T1R family. These two genes were both present in an unpublished microarray from Lopes lab. The microarray analysed the genes specifically expressed in the KV cells of wT and *dld*$^{-/-}$ mutant embryos, which have the Notch signalling affected. In the microarray results, *pkd1* was significantly down regulated in *deltaD*$^{-/-}$ embryos, revealing that *pkd1* transcription might be under the Notch signalling regulation. On the other hand, *tas1r1* was not deferentially regulated by Notch signalling and it had a relatively low expression in wt embryos.

The reasoning that guided us to investigate *tas1r1* role in LR development was a recent publication by Shah *et al* [52] showing that taste receptors surprising have a role in motile cilia, totally unrelated to taste buds[52]. Vertebrates perceive a variety of substances using the two chemosensory systems, taste and olfaction. For taste reception, vertebrates express the two families of G-protein-coupled receptors (GPCRs), T1Rs and T2Rs, in their taste buds [53–56]. Moreover, taste buds also express PLCβ2 and G-protein α-gustducin, which are present in the transduction pathway of taste. Recently, Shah and co-workers discovered that ciliated cells of airway epithelia express multiple T2Rs only in motile cilia and also detected the transcription of PLCβ2 and G-protein α-gustducin in cilia[52]. They speculated that the presence of T2R in airway epithelia is useful to hasten elimination of noxious and harmful substances[52]. In addition, last year, Meyer and colleagues found that *tas1r1* and G-protein α-gustducin, were both expressed in mammalian spermatozoa. These data, raised the possibility that taste receptors act as chemosensors in sperm during the passage through the female reproductive tract[57]. These findings, together with the expression data from our microarray of three other genes that are involved in the taste pathway in taste buds, such as *gnat2, trpm5 and plcβ2* gave us a good reason to investigate the chemosensory hypothesis in the ciliated cells of KV using *tas1r1* as a starting point.

Relatively to *pkd1,* it is described that mutations in both *pkd1* and *pkd2* genes lead to PKD. *pkd1* and *pkd2* codify for two integral membrane proteins, polycystin 1 (Pkd1) and polycistin 2 (Pkd2), respectively[48]. These proteins are localized in primary cilia of kidney cells acting together to form a channel complex where Pkd1 has a long N-terminal extracellular domain, a short C-terminal intracellular domain and eleven transmembranar domains[48]. It was proposed that Pkd1 acts as mechanosensor to detect the bending of each cilium induced by flow stimulation[48,58] and transmits these extracellular signals to Pkd2 through their connecting C-terminal regions[59] (Figure 1.4). It is thought that the signals that Pkd1 senses mechanically, can be transduced into cellular responses that regulate proliferation, adhesion, differentiation and cell morphology[48,58,60]. On the other hand, Pkd2 is a membrane protein

with six transmembranar domains and is a non-selective cation channel that mediates $Ca2^{+}$ influx [48,58], found not only in primary cilia of kidney cells but also in the plasma membrane and in endoplasmic reticulum [59,61,62].

Pkd1 and Pkd2 are unequivocally present in kidney cells primary cilia, but although many authors have also described the presence of Pkd2 in cilia of the mouse node, xenopus node and Kupffer´s vesicle of medaka fish and zebrafish [47,63–67].,the role of the Pkd1-Pkd2 complex in the establishment of the LR axis is still highly debated. Experiments with knockouts and knockdowns of *pkd2* in mice, zebrafish and medaka resulted in kidney cysts and laterally defects in all models [47,63–67]. From these results we can conclude that Pkd2 involvement in the LR establishment is conserved, but how it occurs and which partner it uses in this developmental process has been controversial [29,68,69].

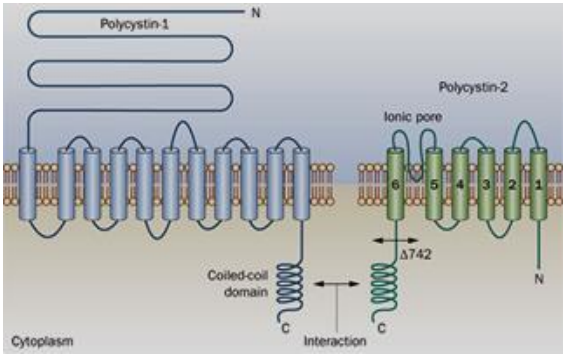

Figure 1.4 Pkd1 - Pkd2 complex at the ciliated kidney cells' membrane
Pkd1 has a large extramembranar domain, responsible for sense the external stimulus. Pkd2 is a transmembranar protein that functions as non-selective cationic channel. Pkd1 and Pkd2 interact via their C-terminal coiled-coil domains faced to the cell cytoplasm.

In mouse nodal cilia and in KV cilia of medaka fish, the presence of Pkd1 has not been reported [67,70]. Moreover, in kidney cells, Pkd1 is required for the localization of Pkd2 in cilia [48] but the same does not happen in mouse node and in kupffer´s vesicle of medaka fish [69,71]. Recent studies developed by Kamura and Field [67,71] revealed that the partner of Pkd2 in the mouse node and in medaka KV is Pkd1l1. Pkd1l1 is also a member of the PKD family of large membrane proteins, which are also known as the TRPP [67].

In summary, in mouse and medaka it is current thought that Pkd1l1 and Pkd2 act together downstream of nodal flow to mediate LR patterning [67,71]. Whether this complex is acting in the cilia membrane or in other cell compartment it has not been formally demonstrated yet. In our microarray we do not have detected expression of *pkd1l1*, but we do have detected *pkd1* transcripts. Our aim was to identify if *pkd1* transcripts code for a true Pkd1 or Pkd1l1, and then study its implication in LR development of the zebrafish embryo.

The zebrafish (*Danio rerio*) is a good vertebrate model in genetic and molecular studies as well as in development. A most important characteristic of this model is the external

fertilization, which allows us to see all steps of embryonic development, since first cellular division, once the embryos are transparent [72]. This transparency also allows the directly visualization of internal organs, such as the KV[73,74]. Moreover, this vertebrate has a relatively short generation span and produces large amounts of eggs [75]. Zebrafish have many mutants, is easily genetically manipulated by gene knockdown and gene overexpression and, as this model has been widely used, there are many transgenic lines reporting genes of interest in several tissues and organs [76,77].

The main goal of this project was to test the two hypothesis of LR determination in the zebrafish embryo.

A. Test the chemosensation hypothesis by knockdown of *tasr1r1* gene.

B. Test the mechanosensation hypothesis by *pkd1* knockdown.

In order to test these hypotheses we tried to abolish the translation of both genes (separately) with morpholino oligonucleotide technology and evaluated the results in the establishment of LR patterning by observation of internal organ position.

2. MATERIAL AND METHODS

In order to answer our proposed objectives, we performed different experiments that are explained bellow.

2.1. Phylogeny

In order to understand if the *pkd1*, present in the microarray, is a *pkd1* gene or a *pkd1l1* gene we did a phylogenetic tree with the protein sequences of these two genes and several other vertebrate organisms, with the help of the IGC Bioinformatics facility.

The protein sequences of *Danio rerio* (Zebrafish) Pkd1 and Pkd1l1 were obtained in Ensemble Genome Browse, and the homologue sequences of other organisms were retrieved from GenBank and Ensemble Genome Browser after BLAST in NCBI. We obtained 15 species, including mouse, human and medaka fish (the number ID is in Table 1 in annex II). Next, we aligned these sequences according to their primary structure similarity using ClustalW [78] with default gap values. The multiple sequence alignment was manually corrected being the numbers of amino acids of all sequences adjusted to the length of the

smallest representative. As outgroup we chose *Drosophila melanogaster*, because is an arthropod. The phylogenetic analysis was inferred from the genetic distance between pairs of sequences using Kimura two parameters method (PROTDIST, Phylip Package, version 3.5c)[79,80] and the tree was constructed by Neighbor Joining (NEIGHBOR, Phylip Package)[81]. The branching order reliability of the tree was evaluated by bootstrap analysis of 1000 replicates.

2.2. Zebrafish mating for embryo production

To obtain embryos, the males and females are collected from a main tank-system and are placed in a matting box in the evening. Each mating box has one male and female separated by a transparent partition to maintain the visual contact. In the following morning the partition is removed the water level is lowered and that triggers a mating ritual between the couple, after which females release the eggs and by external fertilization, the male fertilizes the eggs. As in each mating box there is a grate, the eggs stay protected from the parents, and sink to the bottom of the mating box. After that, the fish go back to the main tank-system, eggs are collected and placed in a Petri dish with embryonic medium (5 mM NaCl, 0.2 mM KCl, 0.3 mM CaCl2, 0.3 mM MgSO4,ddH2O—pH 6.5). The Petri dish with eggs is incubated at 25^{o}C or 28^{o}C until reaching the desired stage for experiments.

2.3. Quantitative Real-Time Polymerase Chain Reaction (qPCR)

The qPCR provides measurement of gene expression and is suitable when a small number of cells are available. In small embryos during in early stages of development qPCR can be very useful.

With *tas1r1*, which had very low expression in the microarray dataset, we wanted to confirm its expression at 10 hpf and 13 hpf. The data obtained at these stages and 4 dpf were normalized using the *elf1a*. After that we decided to compare the *tas1r1* expression at 10 hpf and 13 hpf with its expression at 4dpf. We used this latter stage to compare the levels of transcription because it was described that at 4dpf this gene is highly expressed in the zebrafish mouth, and we wanted to know how much less *tas1r1* expression we had relatively to 4dpf [82].

Relatively to *pkd1*, we compared the levels of gene expression in wt and *deltaD*$^{-/-}$ embryos at bud stage, in order to confirm the microarray data, where this gene was down regulated in *deltaD* mutants. Here, we also normalized the gene expression with reference genes, *elf1a and sox17* at 10 hpf in wt and *deltaD*$^{-/-}$ mutants.

To evaluate the transcription levels and validate our microarray results of *tas1r1* and *pkd1*, we utilized the technique of qPCR in wt and *deltaD* embryos. For *tas1r1* we used wt embryos at 10 hpf (bud stage) and 13 hpf (8 somites stage), while for *pkd1* we only used wt and *deltaD*$^{-/-}$ mutant embryos at 10 hpf because at 13 hpf this gene is also expressed in the zebrafish developing kidney, which would influence the data. For *tas1r1* we performed a positive control of gene expression with cDNA from 4days post fertilization (dpf) when the taste buds are reported to have this receptor expressed.

To perform the qPCR experiments we extracted RNA from 100 embryos of wt and *deltaD*$^{-/-}$ mutants with RNeasy® micro Kit (Qiagen Inc., Valencia, CA) according to the instructions of the manufacture. Next we quantified the RNA obtained in *NanoDrop* 2000 *Spectrophotomer* (Thermo Scientific), a very important step to evaluate the concentration and purity of the RNA. Then we performed the reverse transcription of total RNA samples into cDNA. We used 4 µg of RNA from wt and *deltaD*$^{-/-}$ mutant embryos in a reverse transcription reaction with RevertAid^{TM} First Strand cDNA Synthesis Kit (Fermentas, LIFE SCIENCES), according to the manufactures instructions.

Next, we designed primers for amplification of the cDNAs. We designed primers with the bioinformatic tool Primer-BLAST (NCBI) and primer sequences are described in Table 2.1. The primer sequence of *elf1a*, a house keeping gene used as control, was according to Silva *et al* [83].

Gene	Forward Primer	Reverse Primer	Ta
pkd1	GGGATTCGCTCTCTCACAGG	CACACATCCTGACTGCT	62.3
tas1r1	GTTCTCCGCATGCTCCTTGA	AAAGAGCTCAGCAAAGGCAC	60.3
elf1a	ACGCCTCCTGGCTTTCACCC	TGGGACGAAGGCAACACTGGC	66.1
sox17	GCAAGAGGCTTGCGCAGCAA	CCTGTTTGCGACGCCTGGGT	66.1

Tabela 2.1 Nucleotide sequence of the primers (forward and reverse) used in qPCR assays for each gene in study and respective annealing temperatures (Ta).

The qPCR reactions were performed on the CFX96™ Real-Time PCR Detection System (BIO-RAD PAIS), using Evagreen Supermix (BIO-RAD).

In order to avoid nonspecific annealing and primer-dimmer formation, we tested different annealing temperatures that ranged from 72ºC to 56ºC, as way to determine the optimal annealing temperature for each primer pair. The optimal temperature is chosen based on the lowest Ct value obtained for each primer pair. In the end of this reaction, the program

provides as a melting curve, which shows the specificity of primer annealing. This specificity is represented by a single sharp peak which represents one specific amplicon. If we obtained two sharp peaks in the same melting curve that would mean that we had more than one amplicon being transcribed in the same reaction for the same primer pair. If we obtained two unique peaks in different reaction wells containing the same reaction mix that indicates two different amplicons being obtained with same prime pair.

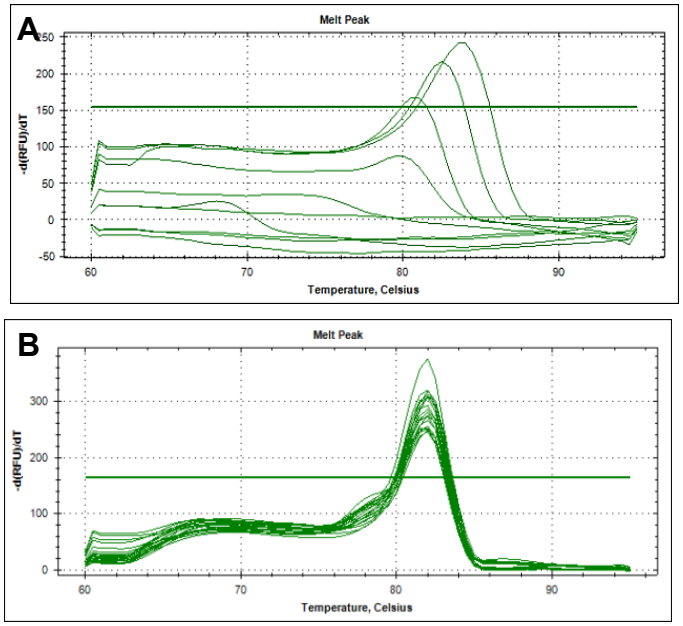

Figure 2.1 qPCR melting curves.
Panel A shows an unspecific primer annealing (with more than one sharp peak) indicating the presence of more than one amplicon. In B, is represented an ideal melting curve with only one sharp peak and, thus, only one amplicon.

In each qPCR reaction for each primer pair we performed a calibration curve with four different concentration of cDNA (1:1, 1:10, 1:100 and 1:1000) with 2 replicates for each concentration. No template control (NTC) reaction was included for each primer pair to test buffers, solutions and DNA contamination and to assess for primer-dimers[84]. Cycling parameters used were as follows: 95°C for 2 min and 95°C for 10s, 62.3°C (for *pkd1*) or 60.3°C (for *tas1R1*) or 66.1°C (for *elf1a* and *sox17*) for 20s in 49 cycles, 60°C for 5s and 95°C for 5s.

We obtained a standard curve which represents the reaction efficiency. This curve is constructed by plotting the log of starting quantity of the template against the Cq values obtained. All data obtained were normalized with the reference gene. Here we utilized the *elf1a* which was described as having an expression very high and maintained along all developmental stages in zebrafish[85]. We also used *sox17* as reference gene for *pkd1* because this gene has a constant expression in bud stage in wt and *deltaD*$^{-/-}$ mutants. Reference genes are important to normalize the data and to correct the differences in amplification by stochastic variation during qPCR.

The data obtained were treated using delta-delta-Cq method available in BIO-RAD software, “BIO-RAD software Manager”.

2.4. Immunofluorescence

We performed an immunofluorescence assay to test if Pkd2 localizes to the cilia in absence of Notch signalling (and presumably in the absence of Pkd1). In order to do that, we used *deltaD*$^{-/-}$ mutant embryos and wt embryos as controls.

The embryos were collected and then were dechorinated at 13 hpf (8 somites stage). After that the embryos were fixed in methanol: DMSO (80:20) during 1 minute. Next, embryos were placed in PBS: Methanol gradually: 75%, 50%, 25% and finally stored in PBS 1x at 4^{o}C and ready to use. Embryos were washed in PBS (250 µl Triton X-100, 10% in 50 ml of PBS and blocked with Foetal Bovine Serum to diminished non-specific binding of primary antibody. Posteriorly, primary antibodies, mouse anti-acetylated α-tubulin (1:400) and rabbit anti-pkd2 (1:400) (a gift from Ian Drummonds’ lab) were incubated in blocking solution (1% DMSO, 2% Foetal Bovine Serum, 0, 1% Tween-20 and PBS) overnight at 4^{o}C.

In the next day embryos were washed in blocking solution and incubated with secondary antibody, anti-mouse *alexa* 546 (1:500) and anti-rabbit *alexa* 488 (1:500) overnight at 4^{o}C. These antibodies have fluorophores which emit green and red light when excited with a wave-length of 488nm and 546 nm respectively.

In the last day, embryos were submitted to several washes and cleared in 50% Glycerol: PBS. Next, embryos were transferred to PBS and stored at 4^{o}C until mounted to confocal microscopy.

Using this antibody we also did an immunofluorescence assay with the transgenic line foxj1a: GFP which has the advantage of having the cells of Kupffer´s vesicle labelled with GFP. The objective of this assay was to test in which type of cilia, Pkd2 co-localizes, immotile or motile. This was done in these transgenic embryos, because *foxj1a* is used as a marker for cells with motile cilia. As fixation in methanol leads to a loss of fluorescence, the embryos were fixed in PFA instead and the block solution was PBDX (50 ml PBS 1x, 0.5g BSA and 0.250 ml 10% Triton X-100). The antibodies used in this assay were the same that I referred above, however we changed the secondary antibody in order to obtain other colour for the visualisation of acetylated tubulin. So we used anti-mouse *alexa* 647 (1:500) and anti-rabbit *alexa* 546 (1:500). The light emitted by these antibodies is magenta and red, respectively.

2.5. Preparation of whole embryos for confocal microscopy

The embryos used in the immunofluorescence assay were flat mounted to visualise the organ of interest – Kupffer´s vesicle with cilia. In a glass slide it was made a circle with silicone and within this circle the embryo was placed in PBS. Finally when the embryo was well orientated, the sample was covered with a lamella and a little pressure was applied to seal the preparation and remove air bubbles. The samples were observed in the confocal microscope - *LSM710 (*ZEISS*)* – with an objective 40X water and 1.2 of numerical aperture and each stack produced slices with 0,4µm -1µm of thickness.

The stacks of images obtained were analysed and treated with the free software "image J" [86].

2.6. Morpholino Injection

Morpholinos (MOs) are synthetic molecules constituted by oligonucleotides that are similar to the structure of natural nucleic acids. Structurally, the difference between morpholinos and DNA is that while morpholinos have standard nucleic acid bases, those bases are bound to morpholino rings instead of deoxyribose rings and linked through phosphorodiamidate groups instead of phosphates. MOs are used to knockdown the expression of proteins by interaction with a complementary mRNA to block its translation to protein or create an alternative splicing site in pre-mRNA. This interaction does not lead to degradation of mRNA and has very few toxic effects.

2.6.1. Morpholino designing

In this experiment we used two different MOs, one of them was to block the translation of *tas1r1* and the other to block *pkd1* translation. However, *pkd1* sequence was not very well annotated, and did not have the initiation codon. Thus, we could not design a MO for the initiation codon to impair the translation of *pkd1* and had designed a MO that binds to an intron-exon boundary to create an alternative splicing site, which according to GeneTools' online advice should lead to an out of frame mutation. As this MO was designed to put exon 3 out of frame, we expected that the protein produced was very small and could be degraded by the proteosome.

We also injected a MO against *pkd2*, as a positive control for our injections, because this morpholino was already described by Schottenfeld *et al.* and causes LR defects in zebrafish embryos [65].

The morpholino for knockdown of *tas1r1* (*tas1r1* augMO) was designed by GeneTools® in order to bind to the mRNA near of its start codon (ATG). Its sequence was:

5´TGCTCAACATCGTTCCCATAATA 3´. As this morpholino binds to an UTR region, the translation is abolished and the protein should not be expressed.

The Morpholino for *pkd1* (*pkd1* splicingMO) was designed to bind to an intron and lead to an alternative splicing site. This interaction should lead to the removal of exon 3 and cause the sequence to go out of frame. The sequence of pkd1 morpholino was: 5´GTACTGTTGGTGACTCACCACAAGT 3´.

The morpholino for knockdown of *pkd2* (*pkd2* augMO) was designed according to Schottenfeld *et al* [65], beginning at the start AUG and extending into the first exon. This morpholino prevents de translation of mRNA to protein, and its sequence was: 5´AGGACGAACGCGACTGGAGCTCATC 3´. Morpholinos arrived lyophilized and then were re-suspend in Milli-Q water, according to the manufacturer's instructions, in order to obtain a final concentration of 1mM stock.

2.6.2. Microinjection of morpholinos

The technique of microinjection is made with precision micro-injectors (Narishigi). These micro-injectors allow injection of very small solution quantities. In these two experiments we injected a range of MO amounts to optimize mortality rates versus phenotypes. We injected: 5.9ng, 9ng, 12ng, 18ng and 24ng for *pkd1* splicingMO at 0.5mM, 0.75mM and 1mM; 1.8ng, 3.5ng, 7ng, 11,9ng and 23ng for *tas1r1* augMO at 0.5mM and 1mM. For *pkd2* augMO we only used 1.8ng at 0.5mM, because this morpholino was already optimized in lab.

The embryos were obtained in the same way, as explained previously, however in this experiment we injected morpholinos at one cell stage. So, when we removed the partition of the matting box, we waited a few minutes for the fish to lay and fertilize the eggs and collected them immediately. Then we put the embryos on the lid of a petri dish that contained a glass-slide and aligned them against the glass-slide to form a string of eggs. Next, we pierced the choreon and the yolk with the sharp needle and injected 1 discharge of MO with a foot pedal device. In the end the embryos were put at 28^{o}C for the next days to evaluate the position of the internal organs, such as heart at 30 hpf, and liver and pancreas at 50 hpf as will be described below.

2.7.Validation for *Pkd1* splicingMO

As *pkd1* splicingMO was a splicing MO, we were able to perform a RT-PCR with cDNA from uninjected and injected embryos, using primers designed before and after the splicing site. This assay should have allowed us to obtain a band in wt embryos of 1080 bp or 1600 bp, for

first and second primer pairs. In contrast in injected embryos we expected to amplify only 917 bp or 1357 bp, respectively.

We did the PCR with My Taq^{TM} Red Mix (BIOLINE) with the following protocol: 95ºC 2min, 95ºC 1min, 61ºC/59ºC (primer pair 1 and 2) 1min, 72º, 2min and 72ºC, 7min.

Gene	Primer pair	Forward Primer	Reverse Primer	Ta
pkd1	1	CAACCAGATCACCACCATCG	CCGTGGTTCATTCACAAAGC	61º
pkd1	2	CAACCAGATCACCACCATCG	GTCTGGAGTTTCGTGTGAGCGC	58º

Tabela 2.2 Nucleotide sequence of the primers (forward and reverse) used in RT-PCR assays and respective annealing temperatures (Ta).

2.8. Evaluation of gut and heart position

After MO injection we wanted to see if there were defects in left-right asymmetry. To access these defects we observed the position of the heart and gut (pancreas and liver), first visualizing under the stereoscope (Nikon, SMZ745) and then by performing an *in situ* hybridization with riboprobes that label these organs unequivocally.

The first organ that appears and allows an evaluation of the effects of the MO is the heart. The heart can be clearly observed at 30 hpf and is positioned on the left side below the left eye in normal embryos. In embryos with laterally defects the heart could be below the right eye or in the middle of the two eyes. At 50 hpf it is already possible to see de gut (liver on the left side and pancreas on the right side). When we want to evaluate gut position we have do previously add PTU (f 1-phenyl 2-thiourea), to the embryo medium, in order to eliminate the pigment (it inhibits melanogenesis by blocking all tyrosinase-dependent steps in the melanin pathway) to facilitate the visualization of internal organs. The evaluation of the gut loop is also possible to do in live embryos when we inject MOs in the transgenic line, sox17:GFP, which has the gut clearly labelled with GFP. These injected transgenic sox17:GFP embryos were scored in the fluorescence stereoscope (*SteREO Discovery.V8* , ZEISS). When the injections were made in wt embryos we performed an in situ hybridization to report the position of both organs.

2.9. Whole mount *in situ* hybridization (WISH)

The *in situ* hybridization allows detection of specific acid nucleic sequences in morphologically preserved cells or embryos. The whole mount in situ hybridization (WISH) normally is used when we want to describe the expression pattern of developmentally

regulated genes[87] . In this methodology we used digoxigenin-labeled antisense RNA probes, which bind to the mRNA of interest in a specific tissue of the embryo.

The probes used to mark the gene expression in the heart and gut were: *cmlc2 (cardiac myosin light chain2)* as a marker of heart position, and *foxA3 (forkhead box A3)* as a marker of gut position. The *in situ* probes used here bound to mRNA specific for these genes in these two organs and allowed us to observe the position and integrity of these organs inside the embryos. These two probes were already available in the lab.

In this experiment we followed the Thisse´s protocol [87]. The embryos injected with MOs were fixed in PFA overnight until the pretended stage (30 hours for the heart and 50 hours for the gut). In the next day, embryos were placed in methanol 100% and stored at -20^{o}C until the first day of the protocol.

In first day the embryos were put through a series of 75%, 50%, 25% MeOH-PBS for 5 min each at RT and then twice for 5 min in PBT (PBS/ Tween20 – 0.1%). Next the embryos were dechorionate and after that were permeabilized with Proteinase K (5mg/ml in PBT) at RT during 30 min or 50 min (time recommend for latter stages). After this step, embryos were fixed in 4% PFA for 20 min, followed by a series of washes in PBT.

The pre-hybridization and hybridization were did at 70ºC for the two ribo-probes in HYB-mix solution (Formamide, 20x SSC, Tween20 10%, 1M citrix acid to pH6 and heparine (0.63mg/ml). After two hours of pre-hybridization, the probes were added to the embryos and incubated overnight.

In the second day the probes were recovered and embryos were submited to 100%, 75%, 50% and 25% of HYB-mix/2x SSC (NaCl 175.3g, Citric acid trisodium salt 88.2g dissolved in 1l of water) washes for 15 min each at 70ºC and then once for 15 min in 2x SSC at 70ºC. After, embryos were washed twice in 0.2 SSC for 30 min and then through 75%, 50% and 25% 0.2 SSC/PBT for 10 min each at RT, finishing with a RT wash in PBT for 10 min. Embryos were blocked for 2 hours at RT with BSA, GS (goat serum) and PBT (50ml PBT with 100mg BSA and 1ml GS). *In situ* hybridization signals were detected at a 1:5000 dilution in blocking solution, overnight at 4ºC.

In the last they, antibody solution was removed and embryos were washed in PBT during 6 series of 15min washes. After that, the embryos were equilibrated in staining buffer (1M TRIS pH9.5, 1M MgCl, 5M NaCl and Tween20 10%), 3 times for 5 min each RT. The color staining was carried out with NBT/BCIP (Roche Mannheim, Germany), alkaline phosphatase subtracts, until probes reached the desired level of purple staining. When the revelation was concluded we stopped the reaction with PFA 4% for 20 min at RT and several washes with

PBT. The embryos were cleared with 50% Glycerol: PBS and photographed in *SteREO Lumar.V12* (ZEISS) with the High Resolution Microscopy Camera AxioCam MRc Rev. 3 FireWire (ZEISS).

2.10. Mounting Zebrafish for Live Imaging

In order to understand if Fox1a is a good marker for motile cilia, we did live imaging using the transgenic line Foxj1a: GFP, which has the KV cells labelled with GFP. To observe all cilia of the KV we injected a construct of mRNA: Arl13b-GFP 400pg. To visualize the KV cilia of the zebrafish embryo we used embryos with 13 hpf and used a mould made with agarose 2% that enables each embryo to stay oriented with KV towards the inverted objective). As live imaging was done in an inverted microscope with the camera recording from the bottom, the embryos, dechorionated, were mounted with the dorsal roof of the KV facing the objective lens – named as "dorsal view". The embryos were obtained as explained initially and are visualized at 13 hpf (8 somites stage). The images were obtained in confocal microscope-*LSM710 (*ZEISS*)* – with an objective 40X water and each stack produced slices with 0,4µm of thickness.

2.11. Statistic analysis

The data analysis was done using the software GraphPad – Prism. The statistical analysis for qPCr and cilia counting cilia in wt and *deltaD*$^{-/-}$ was done with Student's t-test, two tails for two samples assuming unequal variances. We considered values below $p<0.05$ as statistically significant ($p<0.05$ is represented by * and $p< 0.01$ by **)

3. Results and Discussion

To facilitate the description of results I divided the results according to the two different objectives proposed. First I will present the results from objective A: Test the chemosensory pathway using *tas1r1* and then I will discuss the mechanosensory hypothesis with *pkd1.*

A: Test the chemosensory pathway using tas1r1 gene

3.1. Expression of *tas1r1* in cilia of KV at 10 hpf and 13 hpf

The *tas1r1* had a relatively low expression in the microarray screen performed in our lab. However, as the reported expression of this gene in cilia of airway epithelia and sperm was

very surprising and interesting so we decide to test if this gene had some role in LR patterning.

To do that, we evaluated the transcription levels of *tas1r1* in wt embryos at 10 hpf and 13 hpf to confirm its' expression at these stages. The values obtained by q-PCR were normalized relatively to the reference gene, *elf1a* (Figure 3.1).

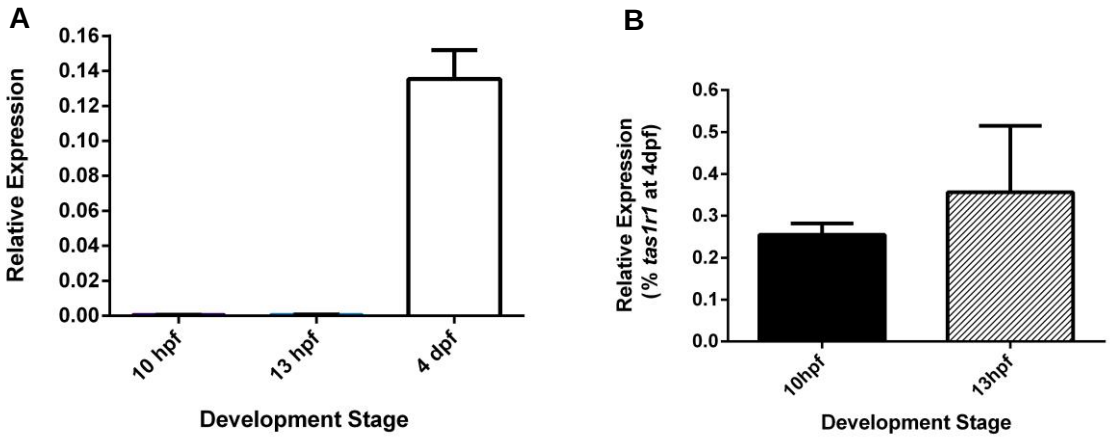

Figure 3.1 Expression analysis of *tas1r1* by qPCR at 10 hpf, 13 hpf and 4 dpf in wt embryos
Gene expression results were normalized with *eif1a* as reference gene **(A and B)** and with gene expression at 4dpf **(B).**

In Figure 3.1A we observed that expression of *tas1r1* at 10 hpf and 13 hpf was very low compared with expression of *tas1r1* at 4 dpf. From this first analysis, we decided to normalize the values with levels of expression of *tas1r1* at 4dpf (Figure 3.1B.) At 4 dpf it was reported that this gene was unequivocally expressed in the mouth of the zebrafish larvae. With this new normalization we can observe that the expression was higher at 13 hpf than at 10 hpf, however this difference was not significant ($p > 0.05$). Moreover, the expression in both stages continued to be very low, between 0.3% and 0.4% (Figure 3.1B).

3.2. Knockdown of *tas1r1* by morpholino injection

We injected different concentrations and amounts of morpholino, to test their toxicity and their effect in LR establishment. After that we evaluated the position of internal organs, such as the heart (at 30 hpf) and gut (50 hpf) to see if *tas1r1* atgMO caused any effects in LR patterning.

For the different MO concentrations and amounts used in this experiment, we did not obtain any laterally defects. The majority (97%-100%) of embryos injected with this morpholino had the heart on the left side of the body as the uninjected control embryos (Figure 3.2)

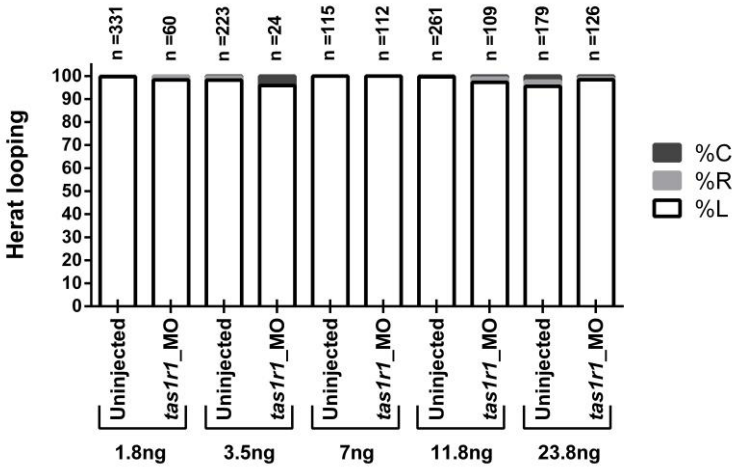

Figure 3.2 Heart laterality of *tas1r1* atgMO injected embryos.
White bars represent the percentage of embryos with the heart on the left side of the body; soft grey bars correspond to percentage of embryos with central heart and dark grey represents the percentage of embryos with hearts on the right side.

We also evaluated the position of gut looping, in normal embryos the liver is on the left side and pancreas on the right side of the body midline (Figure 3.3B). We evaluated the gut position using a transgenic line sox17:GFP that has these organs labelled with GFP. This time, we obtained a few embryos with defects in gut position. We concluded that the *tas1r1* atgMO caused mild gut laterally defects.

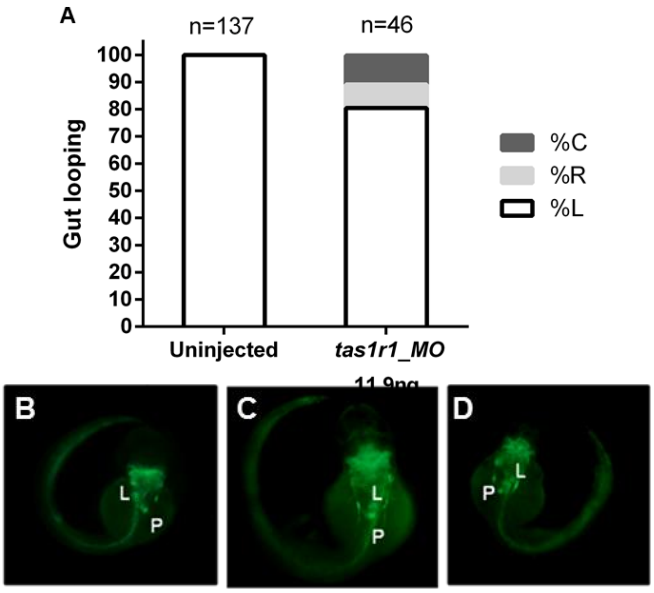

Figure 3.3 Gut laterality in *tas1r1* atgMO injected embryos
White bars represent the percentage of embryos with gut on the left side of the body; soft grey bars correspond to percentage of embryos with central gut and dark grey to the percentage of embryos with gut on the right side **(A).** Fluorescent stereoscope snapshots showing how the gut position was observed in *tas1r1* atgMO transgenic line sox17:GFP. Normal embryo with liver (L) on the left side of body and Pancreas (P) on the right side **(B)**. Embryo without gut looping has central liver and pancreas **(C).** Embryo with reverse gut looping with liver on the right side and pancreas on the left side **(D).**

Once, the anti-Tas1r1 antibodies already tested in zebrafish, are not functional in this model (RL, Personal Communication), we were not able to conclude if this morpholino was in fact blocking translation of the Tas1r1. Moreover, the very low expression in KV cells obtained by microarray and confirmed by qPCR, indicated that this gene was likely not active in the LR process. These results helped us to know that in the microarray, values around 6 (in a scale from 1-15) are not reliable to consider in gene expression studies.

At this stage we cannot rule out the possibility that in the KV cilia there are other genes with the ability to sense chemical stimulus important for correct LR axis body.

B: Test the mechanosensory hypothesis using pkd1 gene

3.3. Phylogenetic study with pkd1 and pkd1l1

The partner of Pkd2 in the mouse node and in the KV cilia of medaka fish, respectively, is Pkd1l1[67,71]**.** However in our microarray *pkd1l1* was not detected in KV cells of zebrafish, only *pkd1*. From this observation we decided to do a phylogenetic study to understand if the *pkd1* transcript present in our microarray was a true *pkd1* or a *pkd1l1*.

The phylogenetic tree is in annex1 – figure 1 and we can distinguish two different clusters. One of them corresponds to Pkd1 and another to Pkd1l1. Moreover, there is a pattern between these two proteins relatively to conservation domains and similarity, because the distribution or arrangement between species is similar into each cluster.

So we concluded that *pkd1* present in our microarray is completely different from *pkd1l1* from medaka fish and mouse, and we performed our studies and experiments with the *pkd1 gene*. However, we cannot exclude the hypothesis that there is also a Pkd1l1 present in the KV cells. This Pkd1l1 was not detected in our microarray, because we did not have a probe for this gene in the Zebrafish Gene Expression 385K Arrays (Roche NimbleGen, Inc., Design ID 090506_Zv7_EXPR).

3.4.Transcriptional levels of *pkd1* in wt and *deltaD*$^{-/-}$ embryos

The expression of *pkd1* in *deltaD*$^{-/-}$ embryos is down regulated relatively to wt embryos. This could mean that *pkd1* is regulated by Notch signalling. To confirm the expression data we did a qPCR experiment at 10 hpf (bud stage) using cDNA from wt and *deltaD*$^{-/-}$ whole embryos to see if this gene was differentially expressed.

Our results showed that *pkd1* was down-regulated in *deltaD*$^{-/-}$ embryos compared with wt embryos, which means that this gene was differentially expressed ($p < 0.05$) confirming the

microarray data. The expression of *pkd1* in *deltaD*$^{-/-}$ embryos was 3.2 times less than in wt embryos.

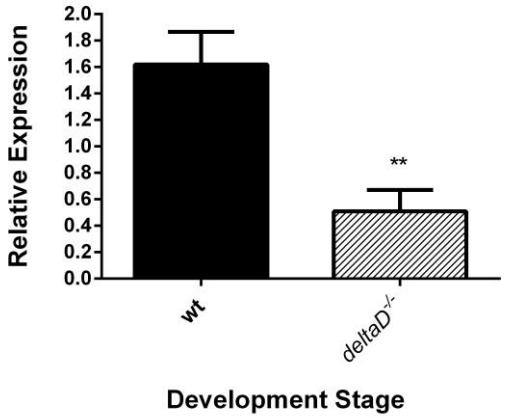

Figure 3.4 Expression analysis of *pkd1* by qPCR in wt and *deltaD*$^{-/-}$ embryos at 10 hpf
Gene expression results were normalized with *elf1*a and *sox17 a*s reference gene. The expression of *pkd1* in *deltaD*$^{-/-}$ mutants was 3.2 times less than *pkd1* expression in wt. p<0.01 (Student´s t-test)

3.5. Knockdown of *pkd1* by morpholino injection

In order to see if the abolishment of *pkd1* in zebrafish causes defects in the establishment of body axis, we injected a morpholino to block the translation of Pkd1. As in *tas1r1* injection, we also saw the position of internal organs to evaluate if the morpholino caused or not laterally defects. We also injected different concentrations and amounts of morpholino to test for toxicity.

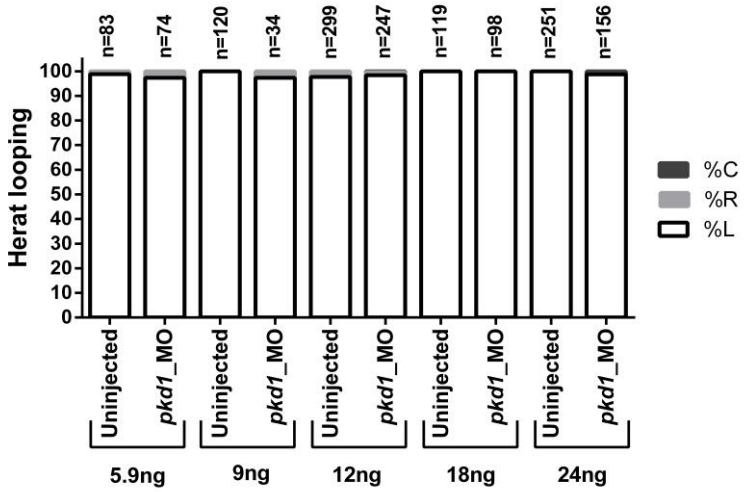

Figure 3.5 Heart laterality of pkd1 splicingMO injected embryos.
White bars represent the percentage of embryos with the heart on the left side of the body; soft grey bars correspond to percentage of embryos with central heart and dark grey represents the percentage of embryos with hearts on the right side

The embryos injected with *pkd1* splicingMO did not show any laterally defects in the different concentrations and amounts used. Most embryos analysed had a normal heart position compared with uninjected embryos, around 98% for all concentrations used (Figure 3.5). The gut looping was also accessed by the transgenic line sox17: GFP. As for the heart position, most of embryos analyzed had normal gut looping (liver on the left side and pancreas on the right side). We also confirmed the gut looping by *in situ* hybridization with *foxA3* probe (Figure 3.6)

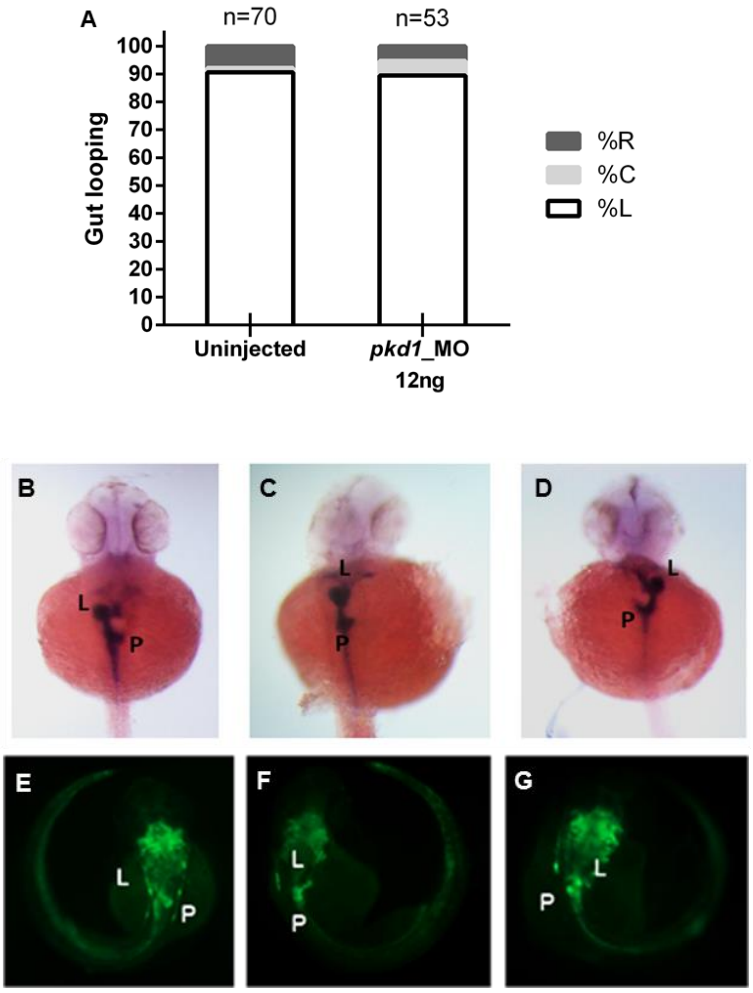

Figure 3.6 Gut laterality in *pkd1* splicingMO injected embryos
White bars represent the percentage of embryos with gut on the left side of the body; soft grey bars correspond to percentage of embryos with central gut and dark grey to the percentage of embryos with gut on the right side **(A).** WISH experiment with foxA3 show the different phenotypes obtained in this experiment **(E-G).** Fluorescent stereoscope snapshots showing how the gut position was observed in *pkd1* splicingMO transgenic line sox17:GFP **(B-D)** Normal embryo with liver (L) on the left side of body and Pancreas (P) on the right side (**B and F).** Embryo without gut looping has central liver and pancreas **(C and F)**. Embryo with reverse gut looping with liver on the right side and pancreas on the left side (**D and G).**

As this morpholino was a splicing morpholino, we tried to do a RT-PCR to confirm if this morpholino was or not functional in our experiments. However we were not able to obtain any expected amplification with all the different primers tested (Figure 2 in annex III).

So, once, we did not obtain any expected result in RT-PCR, we consulted again the Bioinformatics Unit of IGC, to better analyse the information provided by Ensemble Genome Browser (database that we used to take out our sequence) relatively to *pkd1*, we realized that the sequence of this gene was done by projection. This means, that Ensemble Genome Browser used *pkd1* from another species, especially human, to identify the gene structure using *genebuild*. Other useful information was that *pkd1* of zebrafish has only 40% of similarity with human. From this information we concluded that perhaps the sequence annotation was not similar to the real sequence of the *pkd1* gene, which could explain our negative results with the morpholino and RT-PCR. On other hand, we obtained a concordant result in qPCR relatively to our microarray data, which could be explained by the use of a more conserved zone, with better gene annotation. Thereby, we maintain open the hypothesis of Pkd1 acting as a mechanosensor during LR establishment and the possibility of Pkd2 and Pkd1 forming a very important complex during this process.

Other authors described that that there are two different genes, *pkd1a* and *pkd1b* in chromosome1 and 12, respectively. These authors also designed morpholinos against these genes, but did not report any laterally defects[88].

We did a sequence comparison analysis with their morpholinos and we only find matches to a Polycystic 1 like, which is completely different from our sequence. Moreover we tried to find in our sequence their morpholino sequences, but we did not find any similarity. This could mean that there is some incongruence with this gene sequence. All this information could explain our lack of result with the *pkd1* morpholino.

In the LR field and relatively to the mechanosensory hypothesis it has been described that Pkd2 has a crucial role in establishment of LR body axis. As this gene is currently being studied in our lab, we decided to continue studying the mechanosensory hypothesis with *pkd2* gene.

3.6. Injection of *pkd2* morpholino in wt embryos

We injected *pkd2* atgMO, as a positive control morpholino, in order to have a higher confidence in our injections with the others morpholinos, because the defects in LR establishment caused by this pkd2 MO are reported and published in zebrafish[65].

As expected with injection of *pkd2* atgMO, we obtained embryos with laterally defects, in the heart and gut position compared with uninjected embryos. A total of 45% of analysed embryos, showed heart on the left side of the body, 37% had the heart on the right side and 25% had central hearts (Figure 3.7). In addition to laterally defects in the heart, these embryos were also reported to have defects in gut loop position and connective tissue, such as curly tails as reported also by Schottenfeld *et al.*

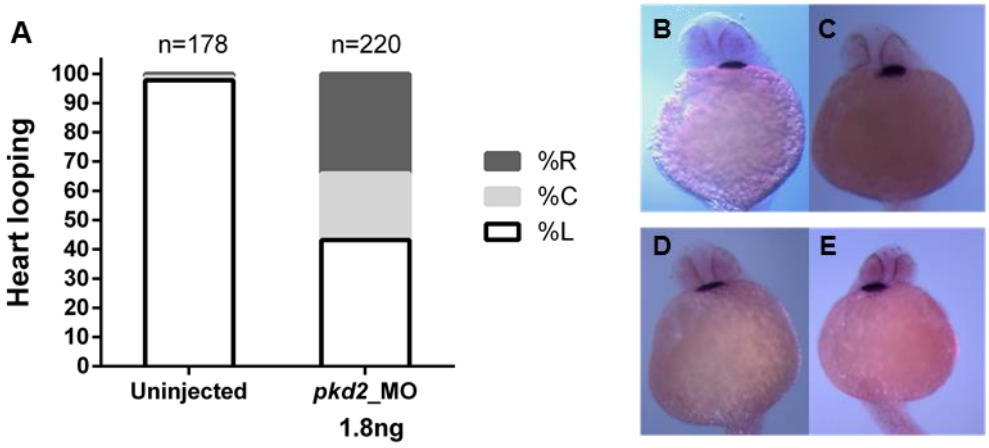

Figure 3.7 Heart laterality of *pkd2* atgMO injeceted embryos
White bars represent the percentage of embryos with heart on the left side of the body; soft grey bars correspond to percentage of embryos with central heart and dark grey to the percentage of embryos with heart on the right side **(A).** WISH experiment with *cmcl2* show the different phenotypes obtained in this experiment **(B-E).** In uninjected embryos the heart looping is on the left side, above the left eye **(B).** Injected embryos could be several phenotypes as left heart jogging **(C)**, no jogging/central position **(D)** or right jogging **(E)**

3.7. Pkd2 localizes to the ciliated KV cells

In order to investigate the localization of Pkd2 in KV ciliated cells we did immunofluorescence in whole mount wt embryos. In these embryos we observed that Pkd2 was present not only in cilia (Figure 3.8) of KV cells, but also in what seems to be the cell membrane and cytoplasm of KV cells (Figure 3.8). Moreover, we observed that sometimes Pkd2 did not localize all over the ciliary length when compared with acetylated α-tubulin that was present throughout the whole cilium (Figure 3.8, see insert).

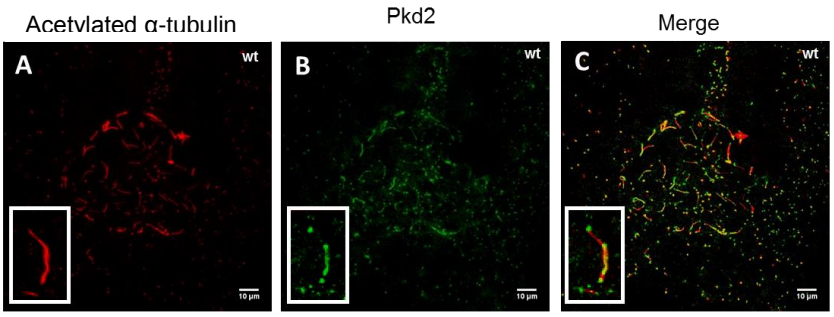

Figure 3.8 Pkd2 Immunostaining in wt embryos
Cilia of Kupffer´s vesicle are shown by confocal microscopy of all z-sections spaced 0.5 µm. Anti-acetylated α-tubulin shows the cilia of KV **(A)** and anti-Pkd2 shows the cilia that have this protein **(B)**. Co-localization between Pkd2 and acetylated α-tubulin **(C)**. Each image has an insert to show that Pkd2 was not present all over the cilium comparatively with acetylated α-tubulin **(C)** White bar - 10µm

We also observed that Pkd2 was not expressed in all KV cilia (Figure 3.9). However we could not detect any asymmetric distribution of Pkd2 positive versus Pkd2 negative cells. These data was interesting because in our lab it was observed that each KV has both immotile and motile cilia (submitted manuscript). By live imaging, labelling cilia with Arl13b: GFP (membrane protein that is present in all cilia) it was possibly to evaluate the number of cilia that is motile and immotile. We thus know that there are 20% of immotile cilia in each wt KV. To understand if the number of Pkd2 positive cilia is coincident with our estimated immotile cilia, and since we do not have a way of reporting Pkd2 in live embryos, we counted the cilia that were both positive for Pkd2 and acetylated α-tubulin per KV (Figure 3.9 and Table 2 in annex IV). The results showed that the percentage of Pkd2 per KV was variable but on average was around 55% of cilia. This value was much higher than the percentage of immotile cilia we had seen before for wt embryos. Therefore we propose that Pkd2 must be localizing not only in immotile cilia, as shown in the mouse, but should be also in some motile cilia.

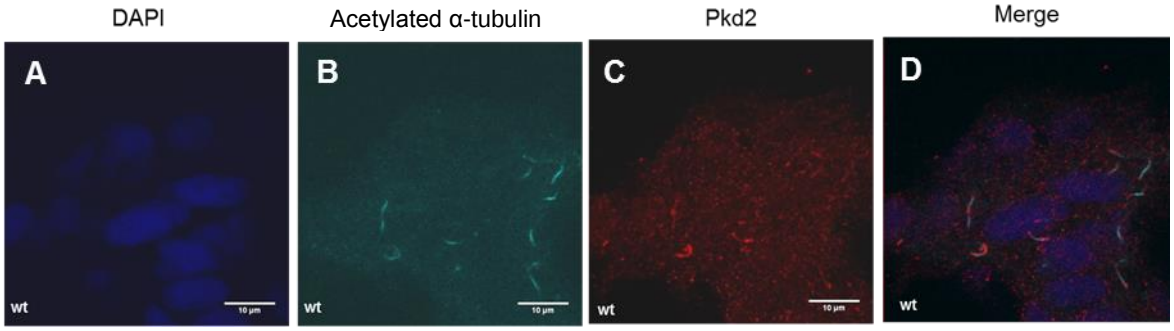

Figure 3.9 Magnification of Pkd2 Immunostaining in wt embryos
Kupffer´s vesicle is shown by confocal microscopy of all z-sections spaced 0.5 µm. The KV cells 'nuclei were labeled with DAPI **(A).** Anti-acetylated α-tubulin labels the KV cilia **(B)** and anti-Pkd2 labels cilia that have this protein **(C)**. There was some co-localization between Pkd2 and acetylated α-tubulin **(D)**. White bar - 10µm

To test this idea we used another transgenic line: foxj1a:GFP that should label all the cells that have this transcription factor, known to be responsible for ciliary motility[89]. In this way we could detect if Pkd2 is present in motile or non-motile ciliated cells.

3.8. Localization of Pkd2 with Foxj1a positive cells.

In this experiment we observed that Pkd2 co-localized with cells positive to Foxj1a:GFP (Figure 3.10). Moreover, with acetylated α-tubulin we observed that all KV cells are positive for Foxj1a. Thus, this experiment told us that all KV cells have at least the potential of having motile cilia (Figure 3.10). But are they all really motile? To answer this question, we did live imaging using the foxj1a: GFP transgenic line injected with Arl13b:GFP (membrane marker, present in all cilia). This experiment definitively showed that Foxj1a is present in cells harbouring both motile and immotile cilia (see Movie 1). Therefore we can determine that Foxj1a is not a definitive marker of motile cilia. Perhaps these cilia have the ability to move but something downstream of Foxj1a must be making them immotile. So, we can conclude that KV cilia can be motile and immotile but both these populations can be Pkd2 positive or negative. We can speculate that perhaps the motile cilia have sensory functions or Pkd2 could be important only as cation channel without any mechanosensor partner and mechanosensory functions.

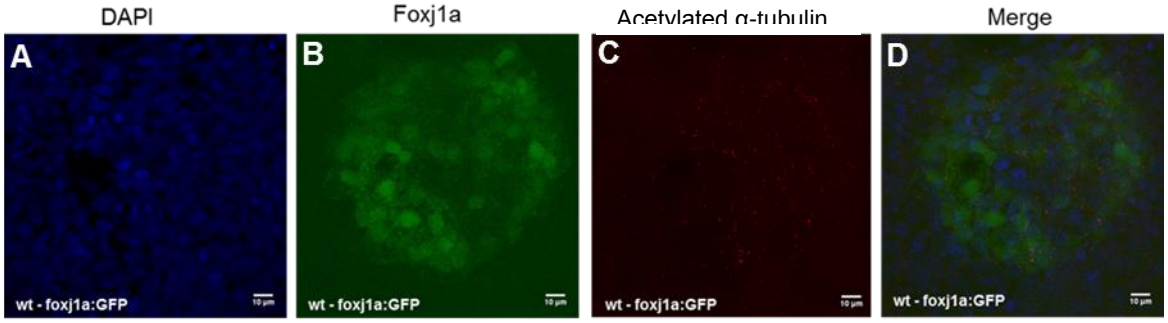

Figure 3.10 All KV cells are positive for foxj1a in wt embryos
Kupffer´s vesicle cilia are shown by confocal microscopy of all z-sections spaced 0.5 µm. The KV cells' nuclei were labeled with DAPI **(A).** The KV cells are labeled with foxj1a:GFP **(B)**. Anti-acetylated α-tubulin labels KV cilia **(C).** Acetylated α-tubulin co-localizes in all foxj1a positive cells **(D)** White bar - 10µm

3.9. Pkd2 does not depend on pkd1 to localize to the cilia

It was reported by Nauli *et al*.[48] that in ciliated kidney cells, Pkd1 is required for the localization of Pkd2[48]. So, as we know that *pkd1* is downregulated in *deltaD*$^{-/-}$ mutants we wanted to understand if in these mutants, Pkd2 still localizes to the cilia. To test this hypothesis we performed an immunofluorescence assay with Pkd2 antibody in *deltaD*$^{-/-}$ embryos.

In this experiment we observed that in *deltaD*$^{-/-}$ embryos, Pkd2 is still able to localize to the cilia (Figure 3.11). We counted the percentage of cilia with and without Pkd2 in wt and *deltaD*$^{-/-}$embryos and the differences were not significant (p> 0.05). This means that, if Pkd1 is really downregulated in *deltaD*$^{-/-}$ embryos then the localization of Pkd2 is not regulated by Notch signalling nor by the absence of Pkd1.

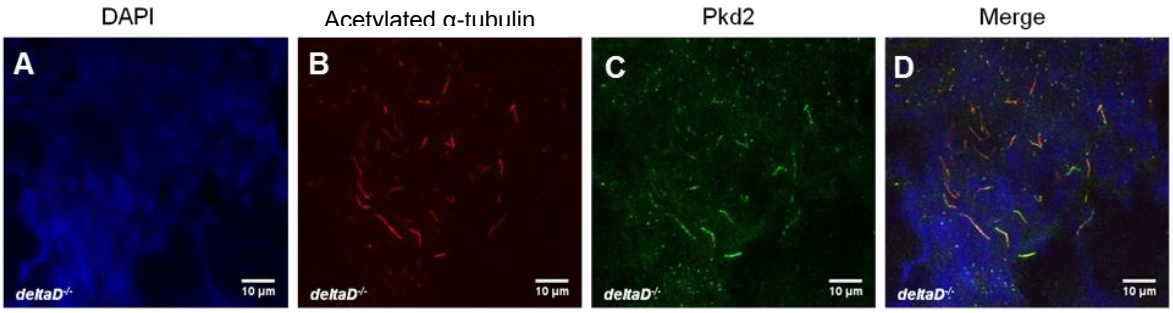

Figure 3.11 Pkd2 Immunostaining in *deltaD*$^{-/-}$ embryos
Kupffer´s vesicle cilia are shown by confocal microscopy of all z-sections spaced 0.5 µm. The KV cells nuclei were labeled with DAPI **(A).** Anti-acetylated α-tubulin labels KV cilia **(B)** and anti-Pkd2 shows the cilia that have this protein **(C)**. There was co-localization between Pkd2 and acetylated α-tubulin **(D)**. White bar - 10µm

3.10. Conclusions future perspective

With this work we concluded that Tas1r1 does not have a role in LR development likely because of its extremely low expression levels in the KV cells. We were unable to definitively characterize if Pkd1 knockdown causes LR defects, because of the poor coverage for this gene in the current Ensemble ZV9.

With the localization study of Pkd2 we discovered that Pkd2 is present in motile and immotile cilia. According to our live imaging experiments using Foxj1a:GFP transgenic embryos injected with Arl13b-GFP these two types of cilia may have the ability to perform similar sensory functions. In light of these findings could be interesting to abolish the immotile cilia genetically and see if motile cilia are sufficient to establish the correct LR axis.

So, for future studies it would be interesting and important to make a construct with Pkd2 tagged to mCherry to inject in Arl13b-GFP transgenic embryos. In this way, with help of live imaging we could observe if Pkd2 localization is really in both types of motile and immotile cilia or in any subset. With the addition of new reporter constructs we hope to be able to understand the reason for Pkd2 localizing in only half of the KV cells.

4. REFERENCES

1. Marshall, W. F. & Nonaka, S. Cilia: tuning in to the cell's antenna. *Curr. Biol.* **16,** R604–14 (2006).

2. Benzing, T. & Schermer, B. Transition zone proteins and cilia dynamics. *Nat. Genet.* **43,** 723–4 (2011).

3. Beales, P. & Jackson, P. K. Cilia - the prodigal organelle. *Cilia* **1,** 1 (2012).

4. Bisgrove, B. W., Makova, S., Yost, H. J. & Brueckner, M. RFX2 is essential in the ciliated organ of asymmetry and an RFX2 transgene identifies a population of ciliated cells sufficient for fluid flow. *Dev. Biol.* **363,** 166–78 (2012).

5. Stephen, L. a *et al.* Failure of centrosome migration causes a loss of motile cilia in talpid(3) mutants. *Dev. Dyn.* (2013). doi:10.1002/dvdy.23980

6. Fisch, C. & Dupuis-Williams, P. Ultrastructure of cilia and flagella - back to the future! *Biol. Cell* **103,** 249–70 (2011).

7. Fliegauf, M., Benzing, T. & Omran, H. When cilia go bad: cilia defects and ciliopathies. *Nat. Rev. Mol. Cell Biol.* **8,** 880–93 (2007).

8. Singla, V. & Reiter, J. F. The primary cilium as the cell's antenna: signaling at a sensory organelle. *Science* **313,** 629–33 (2006).

9. Sloboda, R. D. Intraflagellar transport and the flagellar tip complex. *J. Cell. Biochem.* **94,** 266–72 (2005).

10. Cole, D. G. Novel heterotrimeric kinesin-related protein purified from sea urchin eggs. *Nature* **366,** 268–270 (1993).

11. Kozminski, K. G., Johnson, K. a, Forscher, P. & Rosenbaum, J. L. A motility in the eukaryotic flagellum unrelated to flagellar beating. *Proc. Natl. Acad. Sci. U. S. A.* **90,** 5519–23 (1993).

12. Vincensini, L., Blisnick, T. & Bastin, P. 1001 Model Organisms To Study Cilia and Flagella. *Biol. Cell* **103,** 109–30 (2011).

13. Bisgrove, B. W. & Yost, H. J. The roles of cilia in developmental disorders and disease. *Development* **133,** 4131–43 (2006).

14. Babu, D. & Roy, S. Left-right asymmetry: cilia stir up new surprises in the node. *Open Biol.* **3,** 130052 (2013).

15. Lindemann, C. B. & Lesich, K. a. Flagellar and ciliary beating: the proven and the possible. *J. Cell Sci.* **123,** 519–28 (2010).

16. Ibanez-Tallon, I. To beat or not to beat: roles of cilia in development and disease. *Hum. Mol. Genet.* **12,** 27R–35 (2003).

17. Bloodgood, R. Sensory reception is an attribute of both primary cilia and motile cilia. *J. Cell Sci.* (2010). doi:10.1242/jcs.066308

18. Nonaka, S. *et al.* Randomization of left-right asymmetry due to loss of nodal cilia generating leftward flow of extraembryonic fluid in mice lacking KIF3B motor protein. *Cell* **95,** 829–37 (1998).

19. Goetz, S. C. & Anderson, K. V. The primary cilium: a signalling centre during vertebrate development. *Nat. Rev. Genet.* **11,** 331–44 (2010).

20. Rothschild, S. C., Francescatto, L., Drummond, I. a & Tombes, R. M. CaMK-II is a PKD2 target that promotes pronephric kidney development and stabilizes cilia. *Development* **138,** 3387–97 (2011).

21. Gascue, C., Katsanis, N. & Badano, J. L. Cystic diseases of the kidney: ciliary dysfunction and cystogenic mechanisms. *Pediatr. Nephrol.* **26,** 1181–95 (2011).

22. Fedeles, S. & Gallagher, A. R. Cell polarity and cystic kidney disease. *Pediatr. Nephrol.* **28,** 1161–72 (2013).

23. Wilson, P. D. & Goilav, B. Cystic disease of the kidney. *Annu. Rev. Pathol.* **2,** 341–68 (2007).

24. Mahjoub, M. R., Trapp, M. L. & Quarmby, L. M. NIMA-related kinases defective in murine models of polycystic kidney diseases localize to primary cilia and centrosomes. *J. Am. Soc. Nephrol.* **16,** 3485–9 (2005).

25. Rydholm, S. *et al.* Mechanical properties of primary cilia regulate the response to fluid flow. *Am. J. Physiol. Renal Physiol.* **298,** F1096–102 (2010).

26. Badano, J. L., Mitsuma, N., Beales, P. L. & Katsanis, N. The ciliopathies: an emerging class of human genetic disorders. *Annu. Rev. Genomics Hum. Genet.* **7,** 125–48 (2006).

27. Afzelius, B. A. A human syndrome caused by immotile cilia. *Science* **193,** 317–9 (1976).

28. Afzelius, B. [What happens when the cilia remain immobile?]. *Lakartidningen* **73,** 509–10 (1976).

29. Shiratori, H. & Hamada, H. The left-right axis in the mouse: from origin to morphology. *Development* **133,** 2095–104 (2006).

30. Okada, Y., Takeda, S., Tanaka, Y., Izpisúa Belmonte, J.-C. & Hirokawa, N. Mechanism of nodal flow: a conserved symmetry breaking event in left-right axis determination. *Cell* **121,** 633–44 (2005).

31. Essner, J. J., Amack, J. D., Nyholm, M. K., Harris, E. B. & Yost, H. J. Kupffer's vesicle is a ciliated organ of asymmetry in the zebrafish embryo that initiates left-right development of the brain, heart and gut. *Development* **132,** 1247–60 (2005).

32. Lourenço, R., Lopes, S. S. & Saúde, L. Left-right function of dmrt2 genes is not conserved between zebrafish and mouse. *PLoS One* **5,** e14438 (2010).

33. Sulik, K. *et al.* Morphogenesis of the murine node and notochordal plate. *Dev. Dyn.* **201,** 260–78 (1994).

34. Okabe, N., Xu, B. & Burdine, R. D. Fluid dynamics in zebrafish Kupffer's vesicle. *Dev. Dyn.* **237,** 3602–12 (2008).

35. Bakkers, J., Verhoeven, M. C. & Abdelilah-Seyfried, S. Shaping the zebrafish heart: from left-right axis specification to epithelial tissue morphogenesis. *Dev. Biol.* **330,** 213–20 (2009).

36. Okada, Y. *et al.* Abnormal nodal flow precedes situs inversus in iv and inv mice. *Mol. Cell* **4,** 459–68 (1999).

37. Supp, D. M. *et al.* Targeted deletion of the ATP binding domain of left-right dynein confirms its role in specifying development of left-right asymmetries. *Development* **126,** 5495–504 (1999).

38. El Zein, L., Omran, H. & Bouvagnet, P. Lateralization defects and ciliary dyskinesia: lessons from algae. *Trends Genet.* **19,** 162–7 (2003).

39. Nonaka, S., Shiratori, H., Saijoh, Y. & Hamada, H. Determination of left–right patterning of the mouse embryo by artificial nodal flow. *Nature* **418,** 96–99 (2002).

40. Tanaka, Y., Okada, Y. & Hirokawa, N. FGF-induced vesicular release of Sonic hedgehog and retinoic acid in leftward nodal flow is critical for left-right determination. *Nature* **435,** 172–7 (2005).

41. McGrath, J., Somlo, S., Makova, S., Tian, X. & Brueckner, M. Two populations of node monocilia initiate left-right asymmetry in the mouse. *Cell* **114,** 61–73 (2003).

42. Tabin, C. J. & Vogan, K. J. A two-cilia model for vertebrate left-right axis specification. *Genes Dev.* **17,** 1–6 (2003).

43. Cartwright, J. H. E., Piro, N., Piro, O. & Tuval, I. Embryonic nodal flow and the dynamics of nodal vesicular parcels. *J. R. Soc. Interface* **4,** 49–55 (2006).

44. Sarmah, B., Latimer, A. J., Appel, B. & Wente, S. R. Inositol polyphosphates regulate zebrafish left-right asymmetry. *Dev. Cell* **9,** 133–45 (2005).

45. Cartwright, J. H. E., Piro, O. & Tuval, I. Fluid-dynamical basis of the embryonic development of left-right asymmetry in vertebrates. *Proc. Natl. Acad. Sci. U. S. A.* **101,** 7234–9 (2004).

46. Bataille, S. *et al.* Association of PKD2 (polycystin 2) mutations with left-right laterality defects. *Am. J. Kidney Dis.* **58,** 456–60 (2011).

47. Pennekamp, P. *et al.* The ion channel polycystin-2 is required for left-right axis determination in mice. *Curr. Biol.* **12,** 938–43 (2002).

48. Nauli, S. M. *et al.* Polycystins 1 and 2 mediate mechanosensation in the primary cilium of kidney cells. *Nat. Genet.* **33,** 129–37 (2003).

49. Kawakami, Y. [Mechanisms for establishment of vertebrate left-right asymmetry]. *Tanpakushitsu Kakusan Koso.* **50,** 1609–19 (2005).

50. Francescatto, L., Rothschild, S. C., Myers, A. L. & Tombes, R. M. The activation of membrane targeted CaMK-II in the zebrafish Kupffer's vesicle is required for left-right asymmetry. *Development* **137,** 2753–62 (2010).

51. Christensen, S. T., Pedersen, L. B., Schneider, L. & Satir, P. Sensory cilia and integration of signal transduction in human health and disease. *Traffic* **8,** 97–109 (2007).

52. Shah, A. S., Ben-Shahar, Y., Moninger, T. O., Kline, J. N. & Welsh, M. J. Motile cilia of human airway epithelia are chemosensory. *Science* **325,** 1131–4 (2009).

53. Hoon, M. A. *et al.* Putative mammalian taste receptors: a class of taste-specific GPCRs with distinct topographic selectivity. *Cell* **96,** 541–51 (1999).

54. Adler, E. *et al.* A novel family of mammalian taste receptors. *Cell* **100,** 693–702 (2000).

55. Zhao, G. Q. *et al.* The receptors for mammalian sweet and umami taste. *Cell* **115,** 255–66 (2003).

56. Ishimaru, Y. *et al.* Two families of candidate taste receptors in fishes. *Mech. Dev.* **122,** 1310–21 (2005).

57. Meyer, D. *et al.* Expression of Tas1 taste receptors in mammalian spermatozoa: functional role of Tas1r1 in regulating basal Ca^{2+} and cAMP concentrations in spermatozoa. *PLoS One* **7,** e32354 (2012).

58. Nauli, S. M. & Zhou, J. Polycystins and mechanosensation in renal and nodal cilia. *Bioessays* **26,** 844–56 (2004).

59. Ko, J. Y. & Park, J. H. Mouse models of polycystic kidney disease induced by defects of ciliary proteins. *BMB Rep.* **46,** 73–9 (2013).

60. Chauvet, V. & Tian, X. Mechanical stimuli induce cleavage and nuclear translocation of the polycystin-1 C terminus. *J. Clin. …* **114,** 1433–1443 (2004).

61. Cai, Y. Identification and Characterization of Polycystin-2, the PKD2 Gene Product. *J. Biol. Chem.* **274,** 28557–28565 (1999).

62. Tsiokas, L. Function and regulation of TRPP2 at the plasma membrane. *Am. J. Physiol. Renal Physiol.* **297,** F1–9 (2009).

63. Bisgrove, B. W. Polaris and Polycystin-2 in dorsal forerunner cells and Kupffer´s vesicle are required dor specification of zebrafish left.right axis. (2005).

64. Obara, T. *et al.* Polycystin-2 immunolocalization and function in zebrafish. *J. Am. Soc. Nephrol.* **17,** 2706–18 (2006).

65. Schottenfeld, J., Sullivan-Brown, J. & Burdine, R. D. Zebrafish curly up encodes a Pkd2 ortholog that restricts left-side-specific expression of southpaw. *Development* **134,** 1605–15 (2007).

66. Sun, Z. *et al.* A genetic screen in zebrafish identifies cilia genes as a principal cause of cystic kidney. *Development* **131,** 4085–93 (2004).

67. Kamura, K. *et al.* Pkd1l1 complexes with Pkd2 on motile cilia and functions to establish the left-right axis. *Development* **138,** 1121–9 (2011).

68. Hirokawa, N., Tanaka, Y., Okada, Y. & Takeda, S. Nodal flow and the generation of left-right asymmetry. *Cell* **125,** 33–45 (2006).

69. Karcher, C. *et al.* Lack of a laterality phenotype in Pkd1 knock-out embryos correlates with absence of polycystin-1 in nodal cilia. *Differentiation.* **73,** 425–32 (2005).

70. McGrath, J. Cilia are at the heart of vertebrate left–right asymmetry. *Curr. Opin. Genet. Dev.* **13,** 385–392 (2003).

71. Field, S. *et al.* Pkd1l1 establishes left-right asymmetry and physically interacts with Pkd2. *Development* **138,** 1131–42 (2011).

72. Kimmel, C. B., Ballard, W. W., Kimmel, S. R., Ullmann, B. & Schilling, T. F. Stages of embryonic development of the zebrafish. *Dev. Dyn.* **203,** 253–310 (1995).

73. LopezJimenez, N. D. *et al.* Two members of the TRPP family of ion channels, Pkd1l3 and Pkd2l1, are co-expressed in a subset of taste receptor cells. *J. Neurochem.* **98,** 68–77 (2006).

74. Fishman, M. C., Stainier, D. Y., Breitbart, R. E. & Westerfield, M. Zebrafish: genetic and embryological methods in a transparent vertebrate embryo. *Methods Cell Biol.* **52,** 67–82 (1997).

75. Oike, H. *et al.* Characterization of ligands for fish taste receptors. *J. Neurosci.* **27,** 5584–92 (2007).

76. Yuan, S. & Sun, Z. Microinjection of mRNA and morpholino antisense oligonucleotides in zebrafish embryos. *J. Vis. Exp.* 5–7 (2009). doi:10.3791/1113

77. Sun, Y., Wloga, D. & Dougan, S. T. Embryological manipulations in zebrafish. *Methods Mol. Biol.* **770,** 139–84 (2011).

78. Thompson, J. D., Higgins, D. G. & Gibson, T. J. CLUSTAL W: improving the sensitivity of progressive multiple sequence alignment through sequence weighting, position-specific gap penalties and weight matrix choice. *Nucleic Acids Res.* **22,** 4673–80 (1994).

79. Kimura, M. Journal of Molecular Evolution ©. **16,** (1980).

80. Felsenstein, K. M. & Lewis-Higgins, L. Processing of the beta-amyloid precursor protein carrying the familial, Dutch-type, and a novel recombinant C-terminal mutation. *Neurosci. Lett.* **152,** 185–9 (1993).

81. Saitou, N. & Nei, M. The neighbor-joining method: a new method for reconstructing phylogenetic trees. *Mol. Biol. Evol.* **4,** 406–25 (1987).

82. Hansen, A., Reutter, K. & Zeiske, E. Taste bud development in the zebrafish, Danio rerio. *Dev. Dyn.* **223,** 483–96 (2002).

83. Silva, I. a L., Cancela, M. L. & Conceição, N. Molecular cloning and expression analysis of xpd from zebrafish (Danio rerio). *Mol. Biol. Rep.* **39,** 5339–48 (2012).

84. Taylor, S. *et al.* A Practical Approach to RT-qPCR — Publishing Data That Conform to the MIQE Guidelines. (2009).

85. Nijhof, A. M., Balk, J. A., Postigo, M. & Jongejan, F. Selection of reference genes for quantitative RT-PCR studies in Rhipicephalus (Boophilus) microplus and Rhipicephalus appendiculatus ticks and determination of the expression profile of Bm86. *BMC Mol. Biol.* **10,** 112 (2009).

86. Schneider, C. A., Rasband, W. S. & Eliceiri, K. W. NIH Image to ImageJ: 25 years of image analysis. *Nat. Methods* **9,** 671–5 (2012).

87. Thisse, C. and Thisse, B. High resolution in situ hybridization on whole-mount zebrafish embryo. *Nat. Protoc.* **3,** 59–69 (2008).

88. Mangos, S. *et al.* The ADPKD genes pkd1a/b and pkd2 regulate extracellular matrix formation. *Dis. Model. Mech.* **3,** 354–65 (2010).

89. Yu, X., Ng, C. P., Habacher, H. & Roy, S. Foxj1 transcription factors are master regulators of the motile ciliogenic program. *Nat. Genet.* **40,** 1445–53 (2008).

ANNEXES

Annex I – Phylogenetic tree of Pkd1 and Pkd1l1

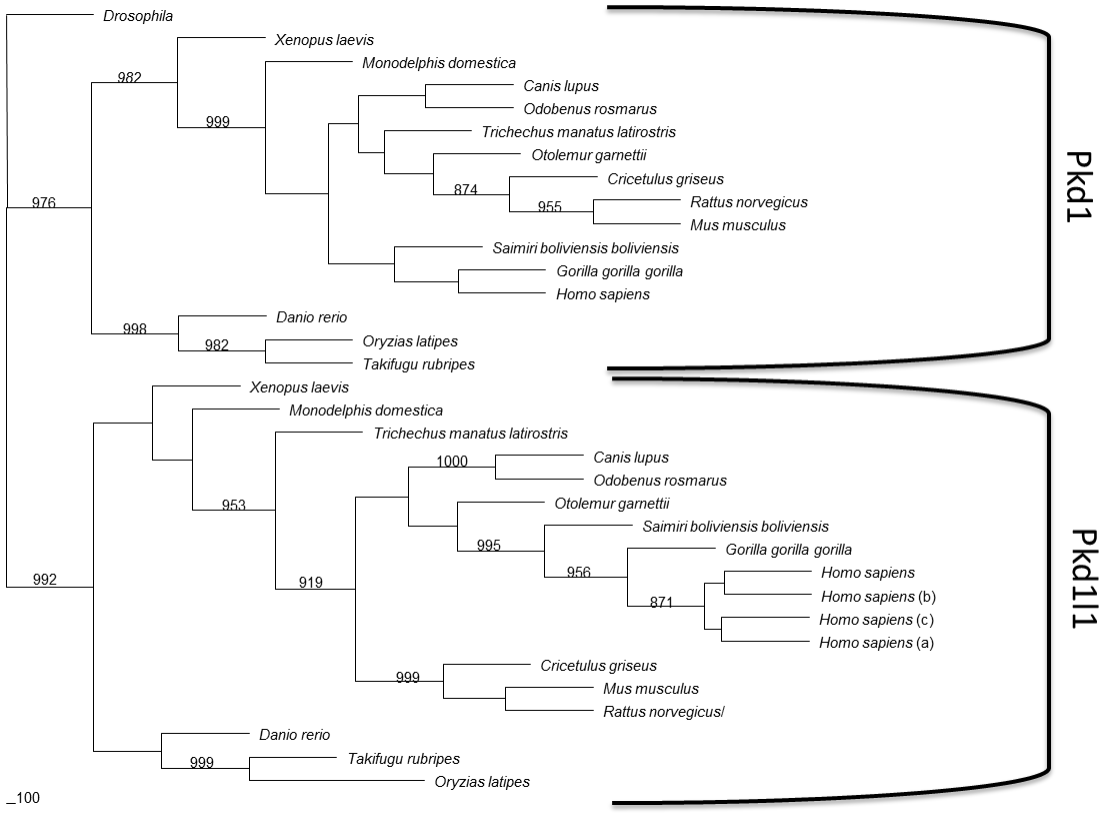

Figure 1. Phylogenetic tree of protein sequence of Pkd1 and Pkd1l1
The tree was constructed by Neighbor Joining (NEIGHBOR, Phylip Package). Only the bootstraps above 800 are represented. The out-group chosen was *Drosophila.*

Annex II – Table with number ID of each protein sequence for Pkd1 and Pkd1l1

	Pkd1 – number ID	Pkd1l1 – number ID
Drosophila	EDW40641.1	Not used
Danio rerio	ENSDART00000039911	ENSDARP00000090175
Xenopus laevis	ENSXETT00000052824	XP_002939619.2
Monodelphis domestica	XP_001366936.2	XM_001379788.2
Canis lupus	AAM45378.1	XM_546847.3
Odobenus rosmarus	XP_004403218.1	XP_004401673.1
Trichechus manatus latirostris	XP_004373451.1	XP_004389521.1
Otolemur garnettii	XP_003790842.1	XP_003797809.1
Cricetulus griseus	XP_003501596.1	EGW04889.1.
Rattus norvegicus	ENSRNOP00000015092	ENSRNOT00000006498
Mus musculus	AAC53207.1	ENSMUSP00000120803
Saimiri boliviensis boliviensis	XP_003928613.1	XP_003930892.1
Gorilla gorilla gorilla	ENSGGOP00000006875	ENSGGOP00000009861
Oryzias latipes	BAG75152.1	BAJ65629.1
Takifugu rubripes	AAB86683.1	ENSTRUP00000013465
Homo sapiens	ENST00000262304	NP_612152.1 EAW61003.1 (isoform - a) EAW61004.1 (isoform - b) EAW61005.1 (isoform - c)

Table 1. Number ID for each protein sequence for Pkd1 and Pkd1l1
From a BLAST,the species were chosen and the numbers ID were obtained in GeneBank and Ensemble

Annex III – Electrophoresis Gel from RT-PCR

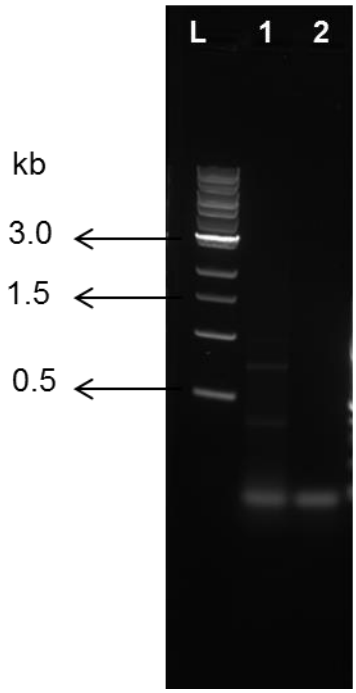

Figure 2. Electrophoresis gel from RT-PCR
We amplify a cDNA control, from wt embryo to test the primes **(1)** and water was used as negative control **(2).** The bands obtained in RT-PCR had not the expected size (1kb).
The ladder used was 1kb

Annex IV – Table with number of cilia co-localizations between acetylated α-tubulin and Pkd2

KV	Number of cilia with acetilated α-tubulin	Number of cilia with Pkd2 and acetylated α-tubulin	Percentage of cilia with Pkd2
1	29	9	31,03
2	42	7	16,67
3	11	3	27,27
4	30	13	43,33
5	56	42	75,00
6	38	9	23,68
7	68	47	69,12
8	20	16	80,00
9	26	9	34,62
10	29	16	55,17
11	44	27	61,36
12	36	13	36,11
13	43	25	58,14
14	88	58	65,91
15	19	8	42,11
16	43	40	93,02
17	55	31	56,36
18	51	40	78,43
19	53	47	88,68
			54,53

Table 2. Number of KV cilia with acetylated α-tubulin and Pkd2
The number of cilia per KV was counted for acetylated α-tubulin and for cilia with acetylated α-tubulin and Pkd2. The percentage of Pkd2 per KV was variable but on average was around 55% of cilia

Annex V

Movie 1. Kupffer's vesicle has both immotile and motile cilia.
Dorsal to ventral view of a Foxj1a:GFP transgenic embryo injected with arl13b-GFP to label all cilia in the Kupffer's vesicle. Both motile and immotile cilia are present inside the KV and both co-localize with foxj1a positive cells. Anterior to the top.